(19) Europäisches Patentamt
European Patent Office
Office européen des brevets

(11) EP 1 722 473 A1

(12) **EUROPEAN PATENT APPLICATION**
published in accordance with Art. 158(3) EPC

(43) Date of publication:
15.11.2006 Bulletin 2006/46

(21) Application number: **05719833.5**

(22) Date of filing: **02.03.2005**

(51) Int Cl.:
H03H 9/145 *(2006.01)* ***H01L 41/09*** *(2006.01)*
H01L 41/18 *(2006.01)* ***H03H 9/25*** *(2006.01)*

(86) International application number:
PCT/JP2005/003518

(87) International publication number:
WO 2005/086345 (15.09.2005 Gazette 2005/37)

(84) Designated Contracting States:
AT BE BG CH CY CZ DE DK EE ES FI FR GB GR HU IE IS IT LI LT LU MC NL PL PT RO SE SI SK TR

(30) Priority: **05.03.2004 JP 2004062921**

(71) Applicant: **MURATA MANUFACTURING CO., LTD.**
Nagaokakyo-shi, Kyoto 617-8555 (JP)

(72) Inventor: **KANDO, Hajime,**
MURATA MANUFACTURING CO., LTD.
Nagaokakyo-shi,
Kyoto 6178555 (JP)

(74) Representative: **Joly, Jean-Jacques**
Cabinet Beau de Loménie
158, rue de l'Université
75340 Paris Cédex 07 (FR)

(54) BOUNDARY ACOUSTIC WAVE DEVICE

(57) To provide a boundary acoustic wave device using SH boundary acoustic waves that has a high electromechanical coupling coefficient, a low propagation loss, a small power flow angle, and a frequency temperature coefficient TCF in an appropriate range, and that has such a simple structure as can be manufactured in a simple process.

The boundary acoustic wave device 1 includes a dielectric body 3 formed over one surface of a $LiTaO_3$ piezoelectric body 2, and an electrode including an IDT 4 and reflectors 5 and 6 at the boundary between the piezoelectric body 2 and the dielectric body 3. The thickness of the electrode is set so that the acoustic velocity of the SH boundary acoustic waves is lower than the acoustic velocities of slow transverse waves propagating in the dielectric body 3 and slow transverse waves propagating in the piezoelectric body 2.

FIG.1

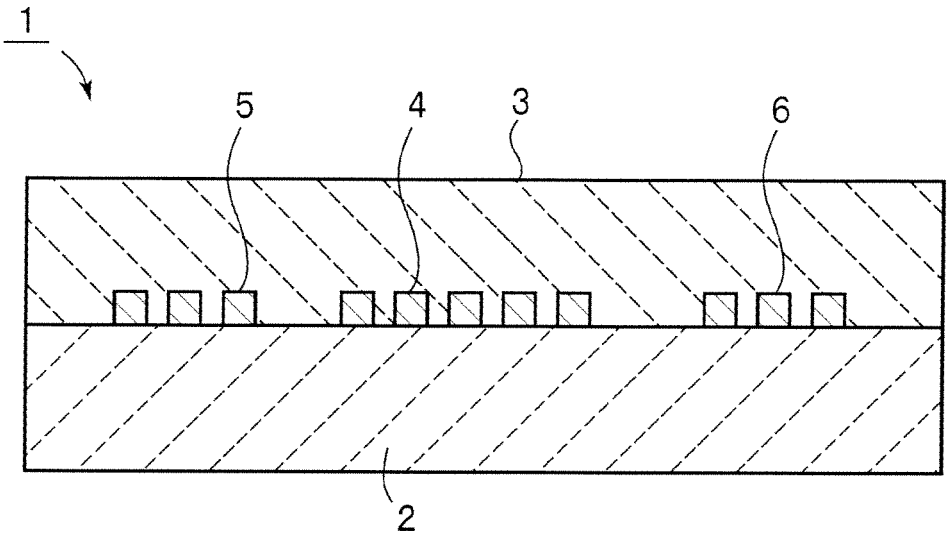

EP 1 722 473 A1

Description

Technical Field

[0001] The present invention relates to boundary acoustic wave devices using SH boundary acoustic waves, and particularly to a boundary acoustic wave device including an electrode disposed at the boundary between a $LiTaO_3$ piezoelectric body and a dielectric body.

Background Art

[0002] A variety of surface acoustic wave devices have been used for cellular phone RF or IF filters, VCO resonators, television VIF filters, and so forth. Surface acoustic wave devices use surface acoustic waves propagating along a surface of a medium, such as Rayleigh waves or first leaky waves.

[0003] Since the surface acoustic waves propagate along a surface of a medium, they are sensitive to the changes of surface conditions. In order to protect the surface of the medium along which surface acoustic waves propagate, the surface acoustic wave element is hermetically enclosed in a package having a cavity in a region opposing the surface acoustic wave-propagating surface of the medium. The package having such a cavity inevitably increases the cost of the surface acoustic wave device. Also, since the package is much larger than the surface acoustic wave element, the resulting surface acoustic wave device must be large.

[0004] In addition to the surface acoustic waves, acoustic waves include boundary acoustic waves propagating along the boundary between solids.

[0005] For example, the below listed Non-Patent Document 1 has disclosed a boundary acoustic wave device including an IDT formed on a 126°-rotated Y-plate X-propagating $LiTaO_3$ substrate, and a SiO_2 layer formed to a predetermined thickness over the IDT and the $LiTaO_3$ substrate. This device propagates SV+P boundary acoustic waves called Stoneley waves. Non-Patent Document 1 has disclosed that when the SiO_2 layer has a thickness of 1.0λ (λ: wavelength of boundary acoustic waves), the electromechanical coupling coefficient is 2%.

[0006] Boundary acoustic waves propagate with their energy concentrated on the boundary between the solids. The bottom surface of the $LiTaO_3$ substrate and the top surface of the SiO_2 film, therefore, hardly have energy, and the characteristics are not varied depending on the changes of the surface conditions of the substrate or the thin layer. Thus, the package having the cavity can be eliminated, and the acoustic wave device can be downsized accordingly.

[0007] The below-listed Non-Patent Document 2 has disclosed SH boundary waves propagating in a [001]-Si(110) /SiO_2/Y-cut X-propagating $LiNbO_3$ structure. This type of SH boundary wave features an electromechanical coupling coefficient K^2 higher than that of the Stoneley waves. In the use of the SH boundary waves as well as in the use of Stoneley waves, the package having the cavity can be eliminated. In addition, since SH boundary waves are of SH-type fluctuation, it can be considered that the strips defining an IDT reflector have a higher reflection coefficient in comparison with the case using Stoneley waves. It is therefore expected that the use of SH boundary waves for, for example, a resonator or a resonator filter can facilitate the downsizing of the device and produce sharp characteristics.

[0008] Non-Patent Document 1: "Piezoelectric Acoustic Boundary Waves Propagating Along the Interface Between SiO2 and LiTaO3" IEEE Trans. Sonics and Ultrason., VOL. SU-25, No. 6, 1978 IEEE

[0009] Non-Patent Document 2: "Highly Piezoelectric Boundary Waves propagating in Si/SiO2/LiNbO3 Structure" (26th EM Symposium, May 1997, pp. 53-58)

[0010] Non-Patent Document 3: "Highly Piezoelectric SH-type Boundary Waves" IEICE Technical Report Vol. 96, No. 249 (US96 45-53) pp. 21-26, 1966

[0011] Non-Patent Document 4: "Production of boundary acoustic wave device by bonding substrate" (in Japanese), Ozawa, Yamada, Omori, Hashimoto, and Yamaguchi, Piezoelectric materials and Device Symposium, 2003, Piezoelectric materials and Device Symposium Executive Committee, Feb. 27, 2003, pp. 59-60

Disclosure of Invention

[0012] A boundary acoustic wave device requires having an electromechanical coupling coefficient of an appropriate magnitude according to the application and exhibiting a low propagation loss, power flow angle, and temperature coefficient of frequency. In addition, low spurious responses are required in the vicinity of the main response.

[0013] Specifically, the loss of boundary acoustic waves accompanied with their propagation, that is, propagation loss adversely affects the insertion loss of the boundary acoustic wave filter, the resonant resistance, and the impedance ratio of the boundary acoustic wave resonator. The impedance ratio is the ratio of the impedance at the resonant frequency to the impedance at the anti-resonant frequency. Hence, the lower the propagation loss, the better.

[0014] The power flow angle represents the difference in direction between the phase velocity of boundary waves and the group velocity of boundary wave energy. If the power flow angle is large, the IDT needs to be disposed at an angle

according to the power flow angle. Accordingly, it is complicated to design the electrode, and a loss resulting from the displacement of the angles is liable to occur.

[0015] The changes in operation frequency with temperature of a boundary wave device reduce the practicable pass band or stop band if the boundary wave device is a boundary wave filter. If the boundary wave device is a resonator, the changes in operation frequency with temperature cause abnormal oscillation in an oscillation circuit. The lower the TCF, which is a change in frequency per degree centigrade, the better.

[0016] A low loss resonator filter may be constructed by, for example, disposing reflectors in the propagation direction outside the region provided with a transmitting and a receiving IDT for transmitting and receiving boundary waves. The bandwidth of the resonator filter depends on the electromechanical coupling coefficient when using the boundary waves. A higher electromechanical coupling coefficient k^2 leads to a broadband filter, and a lower electromechanical coupling coefficient leads to a narrowband filter. Accordingly, it is required that boundary wave devices use an appropriate electromechanical coupling coefficient k^2 according to their applications. For RF filters of cellular phones, the electromechanical coupling coefficient k^2 should be 3% or more, and preferably 5% or more.

[0017] However, in the boundary acoustic wave device disclosed in the above-listed Non-Patent Document 1 using Stoneley waves, the electromechanical coupling coefficient is as low as 2%.

[0018] The object of the present invention is to provide a boundary acoustic wave device using SH boundary waves, exhibiting sufficiently large electromechanical coupling coefficient at the main response, a low propagation loss and power flow angle, a frequency temperature coefficient within the allowable range, and low spurious response of Stoneley waves in the vicinity of the main response.

[0019] A first invention provides a boundary acoustic wave device including a $LiTaO_3$ piezoelectric body, a dielectric body formed over one surface of the piezoelectric body, and an electrode disposed at the boundary between the piezoelectric body and the dielectric body. The electrode satisfies the expression $H > 1.1 \times 10^6\rho^{-1.7}$ when the electrode has a density of ρ (kg/m^3) and a thickness of $H(\lambda)$ and boundary acoustic waves have a wavelength of λ.

[0020] A second invention provides a boundary acoustic wave device includes a $LiTaO_3$ piezoelectric body, a SiO_2 dielectric body formed on one surface of the piezoelectric body, and an electrode disposed at the boundary between the piezoelectric body and the dielectric body. The electrode satisfies the expression $H > 25000\rho^{-1.46}$ when the electrode has a density of ρ (kg/m^3) and a thickness of $H(\lambda)$ and boundary acoustic waves have a wavelength of λ.

[0021] In a specific case of the second invention, the expression $\rho > 2659$ kg/m^3 holds.

[0022] In specific cases of the first and the second invention, the expression $\rho > 4980$ kg/m^3 holds.

[0023] In specific cases of the first and the second invention (hereinafter referred to as the present invention), the electrode includes an electrode layer made of at least one metal selected from the group consisting of Al, Ti, Fe, Cu, Ag, Ta, Au, and Pt.

[0024] In a limited case of the present invention, the electrode further includes a second electrode layer. The second electrode layer made of a different material from the former electrode layer is provided on the upper or lower surface of the former electrode layer.

[0025] In a specific case of the first invention, the dielectric layer is made of a non-piezoelectric material.

[0026] In a specific case of the present invention, the dielectric layer has a multilayer structure including a plurality of dielectric layers.

[0027] In a specific case of the first invention, the dielectric layer is made of at least one selected from the group consisting of Si, SiO_2, glass, SiN, SiC, ZnO, Ta_2O_5, lead zirconate titanate ceramics, AIN, Al_2O_3, $LiTaO_3$, $LiNbO_3$, and potassium niobate (KN).

[0028] In another specific case of the boundary acoustic wave device according to the present invention, the dielectric layer is formed by deposition method.

[0029] In still another specific case, the boundary acoustic wave device according to the present invention further includes a resin layer formed on the surface of the dielectric layer opposite the boundary.

[0030] The boundary acoustic wave device according to the first invention has the dielectric body on one surface of the $LiTaO_3$ piezoelectric body, and the electrode at the boundary between the piezoelectric body and the dielectric body with the expression $H > 1.1 \times 10^6\rho^{-1.7}$ holding. This structure allows the acoustic velocity of SH boundary acoustic waves to be reduced to less than the acoustic velocity of slow transverse waves propagating in the $LiTaO_3$ of the piezoelectric body, and consequently can provide a boundary acoustic wave device using SH boundary waves with a low propagation loss.

[0031] The boundary acoustic wave device according to the second invention has an electrode at the boundary between the $LiTaO_3$ piezoelectric body and the SiO_2 dielectric body with the expression $H > 25000\rho^{-1.46}$ holding. This structure allows the acoustic velocity of SH boundary waves propagating along the boundary between the $LiTaO_3$ and the SiO_2 to be reduced to less than the acoustic velocity of transverse waves propagating in the SiO_2, and consequently can provide a boundary acoustic wave device using SH boundary acoustic waves that exhibits a low propagation loss in spite of a leaking type.

[0032] In the second invention, if the ρ is higher than 2659 kg/m^3, the electrode thickness H can be reduced to 0.25λ

or less, the electrode thickness allowing the velocity of the SH boundary waves to be reduced to less than that of the slow transverse waves propagating in the SiO_2. Thus, the electrode can be easily formed by thin layer deposition method.

[0033] In the present invention, the electrode made of at least one metal selected from the group consisting of Al, Ti, Fe, Cu, Ag, Ta, Au, and Pt ensures the production of a boundary wave device using SH boundary waves according to the present invention. If the electrode further includes a second electrode layer made of a different metal from the above electrode layer, the adhesion between the electrode and the dielectric body or $LiTaO_3$ or the electric power resistance can be enhanced by appropriately selecting the metal forming the second electrode.

[0034] The dielectric body may be piezoelectric, and preferably contain SiO_2 as the principal constituent. A SiO_2 dielectric body can improve the temperature coefficient of the frequency.

[0035] In the present invention, the dielectric body may have a multilayer structure including a plurality of dielectric layers. In this instance, the dielectric layers can be formed of a variety of dielectric materials.

[0036] In the first invention, by forming the dielectric layer of at least one selected from the group consisting of Si, SiO_2, glass, SiN, SiC, Al_2O_3, ZnO, Ta_2O_5, lead zirconate titanate ceramics, AIN, $LiTaO_3$, $LiNbO_3$, and potassium niobate (KN), a boundary wave device using SH boundary waves can be achieved according to the present invention.

[0037] In addition, by using at least one non-piezoelectric material selected from the group consisting of Si, SiO_2, glass, SiN, SiC, and Al_2O_3 as the material of the dielectric layer, the dielectric layer can be stably formed by deposition method, because the dielectric layer is not affected by the nonuniformity of the piezoelectric characteristics of the dielectric layer.

[0038] In the formation of the dielectric layer of the present invention, for example, if the substrate bonding method disclosed in Non-Patent Document 4 is applied for bonding the $LiTaO_3$ and the dielectric body together, the boundary waves may be nonuniformly propagated due to the nonuniformity of the bonded region. Accordingly, critical defects occur in practice, such as significantly large deviation in frequency, variation in insertion loss of filters, variation in resonant resistance of resonators. In addition, in order to obtain a strength to prevent the substrate from breaking in the manufacturing process, the dielectric layer and the $LiTaO_3$ that are to be bonded together have to have thicknesses of, for example, at least 300 μm. Accordingly, the resulting device is as thick as 600 μm in total. In the present invention, a deposition method, such as a sputtering method, a vapor deposition method, or a CVD method (chemical vapor deposition method), is preferably applied instead of the bonding method. The deposition method facilitates the formation of a uniform, thin layer over the entire surface of a substrate, and leads to a more uniform frequency, insertion loss, and resonant resistance than the bonding method. The deposition method allows the thickness of the dielectric layer to be about 2λ with the $LiTaO_3$ having a thickness of, for example, 300 μm to maintain the strength. For example, the dielectric layer can have a thickness as small as about 10 μm for boundary waves with a wavelength λ of 5 μm. Thus, the thickness of the resulting device can be reduced to 310 μm in total, that is, to half the device produced using the bonding method.

[0039] In the present invention, if a resin layer is formed on the surface of the dielectric layer opposite the boundary, the moisture resistance can be enhanced by appropriately selecting the material.

Brief Description of the Drawings

[0040]

Fig. 1 is a front sectional view of a boundary acoustic wave device according to an embodiment of the present invention.

Fig. 2 is a plot showing the relationship between the thickness of a Au electrode and the acoustic velocity V of some types of waves in a structure including the Au electrode and a SiO_2 layer on a (0°, 90°, 0°) $LiTaO_3$ substrate.

Fig. 3 is a plot showing the relationship between the thickness of the Au electrode and the electromechanical coupling coefficient k^2 of SH boundary waves (U2) in the structure including the Au electrode and the SiO_2 layer on the (0°, 90°, 0°) $LiTaO_3$ substrate.

Fig. 4 is a plot showing the relationship between the thickness of the Au electrode and the propagation loss α of SH boundary waves (U2) in the structure including the Au electrode and the SiO_2 layer on the (0°, 90°, 0°) $LiTaO_3$ substrate.

Fig. 5 is a plot showing the relationship between the thickness of the Au electrode and the frequency temperature coefficient TCF of SH boundary waves (U2) in the structure including the Au electrode and the SiO_2 layer on the (0°, 90°, 0°) $LiTaO_3$ substrate.

Fig. 6 is a plot showing the relationship between the thickness of the Au electrode and the power flow angle PFA of SH boundary waves (U2) in the structure including the Au electrode and the SiO_2 layer on the (0°, 90°, 0°) $LiTaO_3$ substrate.

Fig. 7 is a plot showing the relationship between the thickness of the Au electrode and the acoustic velocity V of some types of waves in the structure including the Au electrode and the SiO_2 layer on the (0°, 90°, 0°) $LiTaO_3$ substrate.

Fig. 8 is a plot showing the relationship between the thickness of the Au electrode and the electromechanical coupling coefficient k^2 of Stoneley wave (U3) in the structure including the Au electrode and the SiO_2 layer on the (0°, 90°, 0°) $LiTaO_3$ substrate.

Fig. 9 is a plot showing the relationship between the thickness of the Au electrode and the propagation loss α of Stoneley wave (U3) in the structure including the Au electrode and the SiO_2 layer on the (0°, 90°, 0°) LiTa03 substrate.

Fig. 10 is a plot showing the relationship between the thickness of the Au electrode and the frequency temperature coefficient TCF of Stoneley wave (U3) in the structure including the Au electrode and the SiO_2 layer on the (0°, 90°, 0°) $LiTaO_3$ substrate.

Fig. 11 is a plot showing the relationship between the thickness of the Au electrode and the power flow angle PFA of Stoneley wave (U3) in the structure including the Au electrode and the SiO_2 layer on the (0°, 90°, 0°) $LiTaO_3$ substrate.

Fig. 12 is a plot showing the relationship between the thickness of the Au electrode and the acoustic velocity V of some types of waves in the structure including the Au electrode and the SiO_2 layer on the (0°, 90°, 0°) $LiTaO_3$ substrate.

Fig. 13 is a plot showing the relationship between the thickness of the Au electrode and the electromechanical coupling coefficient k^2 of longitudinal boundary waves (U1) in the structure including the Au electrode and the SiO_2 layer on the (0°, 90°, 0°) $LiTaO_3$ substrate.

Fig. 14 is a plot showing the relationship between the thickness of the Au electrode and the propagation loss α of longitudinal boundary waves (U1) in the structure including the Au electrode and the SiO_2 layer on the (0°, 90°, 0°) $LiTaO_3$ substrate.

Fig. 15 is a plot showing the relationship between the thickness of the Au electrode and the frequency temperature coefficient TCF of longitudinal boundary waves (U1) in the structure including the Au electrode and the SiO_2 layer on the (0°, 90°, 0°) $LiTaO_3$ substrate.

Fig. 16 is a plot showing the relationship between the thickness of the Au electrode and the power flow angle PFA of longitudinal boundary waves (U1) in the structure including the Au electrode and the SiO_2 layer on the (0°, 90°, 0°) $LiTaO_3$ substrate.

Fig. 17 is a plot showing the relationship between the thickness of the Au electrode and the acoustic velocity V of SH boundary waves in the structure including the Au electrode and the SiO_2 layer on the (0°, 90°, 0°) $LiTaO_3$ substrate.

Fig. 18 is a plot showing the relationship between the thickness of the Au electrode and the propagation loss α of SH boundary waves (U2) in the structure including the Au electrode and the SiO_2 layer on the (0°, 90°, 0°) $LiTaO_3$ substrate.

Fig. 19 is a plot showing the relationship between the thickness of the Au electrode and the frequency temperature coefficient TCF of SH boundary waves (U2) in the structure including the Au electrode and the SiO_2 layer on the (0°, 90°, 0°) $LiTaO_3$ substrate.

Fig. 20 is a plot showing the relationship between the thickness of the Au electrode and the power flow angle PFA of SH boundary waves (U2) in the structure including the Au electrode and the SiO_2 layer on the (0°, 90°, 0°) $LiTaO_3$ substrate.

Fig. 21 is a plot showing the relationship between the thickness of a Cu electrode and the acoustic velocity V of SH boundary waves in a structure including the Cu electrode and a SiO_2 layer on a (0°, 90°, 0°) $LiTaO_3$ substrate.

Fig. 22 is a plot showing the relationship between the thickness of the Cu electrode and the propagation loss α of SH boundary waves (U2) in the structure including the Cu electrode and the SiO_2 layer on the (0°, 90°, 0°) $LiTaO_3$ substrate.

Fig. 23 is a plot showing the relationship between the thickness of the Cu electrode and the frequency temperature coefficient TCF of SH boundary waves (U2) in the structure including the Cu electrode and the SiO_2 layer on the (0°, 90°, 0°) $LiTaO_3$ substrate.

Fig. 24 is a plot showing the relationship between the thickness of the Cu electrode and the power flow angle PFA of SH boundary waves (U2) in the structure including the Cu electrode and the SiO_2 layer on the (0°, 90°, 0°) $LiTaO_3$ substrate.

Fig. 25 is a plot showing the relationship between the thickness of an Al electrode and the acoustic velocity V of SH boundary waves in a structure including the Al electrode and a SiO_2 layer on a (0°, 90°, 0°) $LiTaO_3$ substrate.

Fig. 26 is a plot showing the relationship between the thickness of the Al electrode and the propagation loss α of SH boundary waves (U2) in the structure including the Al electrode and the SiO_2 layer on the (0°, 90°, 0°) $LiTaO_3$ substrate.

Fig. 27 is a plot showing the relationship between the thickness of the Al electrode and the frequency temperature coefficient TCF of SH boundary waves (U2) in the structure including the Al electrode and the SiO_2 layer on the (0°, 90°, 0°) $LiTaO_3$ substrate.

Fig. 28 is a plot showing the relationship between the thickness of the Al electrode and the power flow angle PFA of SH boundary waves (U2) in the structure including the Al electrode and the SiO_2 layer on the (0°, 90°, 0°) $LiTaO_3$

substrate.

Fig. 29 is a plot showing the relationship between the thickness of a Ag electrode and the acoustic velocity V of SH boundary waves V in a structure including the Ag electrode and a SiO_2 layer on a (0°, 90°, 0°) $LiTaO_3$ substrate.

Fig. 30 is a plot showing the relationship between the thickness of the Ag electrode and the propagation loss α of SH boundary waves (U2) in the structure including the Ag electrode and the SiO_2 layer on the (0°, 90°, 0°) $LiTaO_3$ substrate.

Fig. 31 is a plot showing the relationship between the thickness of the Ag electrode and the frequency temperature coefficient TCF of SH boundary waves (U2) in the structure including the Ag electrode and the SiO_2 layer on the (0°, 90°, 0°) $LiTaO_3$ substrate.

Fig. 32 is a plot showing the relationship between the thickness of the Ag electrode and the power flow angle PFA of SH boundary waves (U2) in the structure including the Ag electrode and the SiO_2 layer on the (0°, 90°, 0°) $LiTaO_3$ substrate.

Fig. 33 is a plot showing the relationship between the thickness of an Fe electrode and the acoustic velocity V of SH boundary waves in a structure including the Fe electrode and a SiO_2 layer on a (0°, 90°, 0°) $LiTaO_3$ substrate.

Fig. 34 is a plot showing the relationship between the thickness of the Fe electrode and the propagation loss α of SH boundary waves (U2) in the structure including the Fe electrode and the SiO_2 layer on the (0°, 90°, 0°) $LiTaO_3$ substrate.

Fig. 35 is a plot showing the relationship between the thickness of the Fe electrode and the frequency temperature coefficient TCF of SH boundary waves (U2) in the structure including the Fe electrode and the SiO_2 layer on the (0°, 90°, 0°) $LiTaO_3$ substrate.

Fig. 36 is a plot showing the relationship between the thickness of the Fe electrode and the power flow angle PFA of SH boundary waves (U2) in the structure including the Fe electrode and the SiO_2 layer on the (0°, 90°, 0°) $LiTaO_3$ substrate.

Fig. 37 is a plot showing the relationship between the thickness of a Pt electrode and the acoustic velocity V of SH boundary waves in a structure including the Pt electrode and a SiO_2 layer on a (0°, 90°, 0°) $LiTaO_3$ substrate.

Fig. 38 is a plot showing the relationship between the thickness of the Pt electrode and the propagation loss α of SH boundary waves (U2) in the structure including the Pt electrode and the SiO_2 layer on the (0°, 90°, 0°) $LiTaO_3$ substrate.

Fig. 39 is a plot showing the relationship between the thickness of the Pt electrode and the frequency temperature coefficient TCF of SH boundary waves (U2) in the structure including the Pt electrode and the SiO_2 layer on the (0°, 90°, 0°) $LiTaO_3$ substrate.

Fig. 40 is a plot showing the relationship between the thickness of the Pt electrode and the power flow angle PFA of SH boundary waves (U2) in the structure including the Pt electrode and the SiO_2 layer on the (0°, 90°, 0°) $LiTaO_3$ substrate.

Fig. 41 is a plot showing the relationship between the thickness of a Ti electrode and the acoustic velocity V of SH boundary waves in a structure including the Ti electrode and a SiO_2 layer on a (0°, 90°, 0°) $LiTaO_3$ substrate.

Fig. 42 is a plot showing the relationship between the thickness of the Ti electrode and the propagation loss α of SH boundary waves (U2) in the structure including the Ti electrode and the SiO_2 layer on the (0°, 90°, 0°) $LiTaO_3$ substrate.

Fig. 43 is a plot showing the relationship between the thickness of the Ti electrode and the frequency temperature coefficient TCF of SH boundary waves (U2) in the structure including the Ti electrode and the SiO_2 layer on the (0°, 90°, 0°) $LiTaO_3$ substrate.

Fig. 44 is a plot showing the relationship between the thickness of the Ti electrode and the power flow angle PFA of SH boundary waves (U2) in the structure including the Ti electrode and the SiO_2 layer on the (0°, 90°, 0°) $LiTaO_3$ substrate.

Fig. 45 is a plot showing the relationship between the thickness of a Ta electrode and the acoustic velocity V of SH boundary waves in a structure including the Ta electrode and a SiO_2 layer on a (0°, 90°, 0°) $LiTaO_3$ substrate.

Fig. 46 is a plot showing the relationship between the thickness of the Ta electrode and the propagation loss α of SH boundary waves (U2) in the structure including the Ta electrode and the SiO_2 layer on the (0°, 90°, 0°) $LiTaO_3$ substrate.

Fig. 47 is a plot showing the relationship between the thickness of the Ta electrode and the frequency temperature coefficient TCF of SH boundary waves (U2) in the structure including the Ta electrode and the SiO_2 layer on the (0°, 90°, 0°) $LiTaO_3$ substrate.

Fig. 48 is a plot showing the relationship between the thickness of the Ta electrode and the power flow angle PFA of SH boundary waves (U2) in the structure including the Ta electrode and the SiO_2 layer on the (0°, 90°, 0°) $LiTaO_3$ substrate.

Fig. 49 is a plot showing the relationship between the density of electrode materials and the thickness at which the acoustic velocity of SH boundary waves is reduced to less than that of transverse waves.

Reference Numerals

[0041]

1: boundary acoustic wave device
2: piezoelectric body
3: dielectric body
4: IDT serving as electrode
5, 6: reflector serving as electrode

Best Mode for Carrying Out the Invention

[0042] The present invention will be apparent from the following description of embodiments of the present invention with reference to the drawings.

[0043] In order to propagate boundary acoustic waves between two solid layers, it is necessary to satisfy the requirements for concentrating the energy of boundary waves on the boundary between the solid layers. For this purpose, Non-Patent Document 3 has disclosed a method in which a material is selected which allows the transverse wave velocity in a BGSW substrate to be close to the transverse wave velocity in an isotropic material and has a low density ratio to the isotropic material, and moreover which is high -piezoelectric, as described above. When a material has a high velocity region and a low velocity region, waves are propagated concentrating on the low acoustic velocity region. The present inventors have found that the requirements for concentrating the energy on the boundary between the solid layers are satisfied by using a metal having a high density and a low acoustic velocity, such as Au, for an electrode disposed between the two solid layers, and by increasing the thickness of the electrode to reduce the acoustic velocity of the boundary waves propagating between the solid layers. Thus, the present invention has been accomplished.

[0044] It has been known that bulk waves propagating in a solid material include three type waves: longitudinal waves; fast transverse waves; and slow transverse waves, which are called P waves, SH waves, and SV waves respectively. Which waves of the SH waves and the SV waves are slow depends on the anisotropy of the substrate. The bulk waves having the lowest acoustic velocity of these three type bulk waves are the slow transverse waves. If the solid material is isotropic like SiO_2, a single type of transverse waves propagates. In this instance, this type of transverse waves is the slow transverse waves.

[0045] Boundary acoustic waves propagating along an anisotropic substrate, such as a piezoelectric substrate, generally propagate with the three displacement components combined: P waves, SH waves, and SV waves, and the principal component determines the type of the boundary acoustic waves. For example, the above-mentioned Stoneley waves are boundary acoustic waves mainly including P waves and SV waves, and SH boundary waves mainly include SH waves. The SH waves and the P or SV waves may propagate without combining with each other in some cases.

[0046] Since boundary acoustic waves propagate with the three displacement components combined with each other, boundary acoustic waves, for example, with a higher acoustic velocity than SH waves leak the SH-wave and SV-wave components. Boundary acoustic waves with a higher acoustic velocity than SV waves also leak the SV-wave component. These leaked components cause the propagation loss of the boundary waves.

[0047] Accordingly, by reducing the acoustic velocity of the SH boundary waves to less than the acoustic velocities of slow transverse waves in the two solid layers, the energy of the SH boundary waves can be concentrated on the electrode disposed between the two solid layers, and thus SH boundary waves with a high electromechanical coupling coefficient k^2 can be propagated. Thus, the requirements for making the propagation loss zero are satisfied. The present invention is based on this concept.

[0048] In addition, by designing the two solid layers such that at least one of the solid layers is made of a piezoelectric body and the other solid layer is made of a dielectric body containing a piezoelectric material, the electrode between the solid layers excites SH boundary waves. In this instance, a comb-like or Japanese bamboo screen-like electrode (interdigital transducer, IDT) can be used as the electrode, as described in, for example, "Introduction of surface acoustic wave (SAW) device simulation" (in Japanese, Hashimoto, Realize Corp., p. 9).

[0049] Fig. 1 is a schematic front sectional view of a boundary acoustic wave device according to an embodiment of the present invention. The boundary acoustic wave device 1 includes a piezoelectric body 2 made of $LiTaO_3$ plate and a dielectric body 3 formed on the piezoelectric body. An IDT 4 and reflectors 5 and 6 are disposed as the electrode at the boundary between the piezoelectric body 2 and the dielectric body 3. The reflectors 5 and 6 are located on both sides in the surface wave propagation direction of the IDT 4. Thus, the present embodiment structures a boundary wave resonator.

[0050] The boundary acoustic wave device 1 of the present embodiment features the thickness of the electrode, that is, the IDT 4 and the reflectors 5 and 6. Specifically, the thickness of the electrode is set so that the acoustic velocity of SH boundary acoustic waves is lower than the acoustic velocities of slow transverse waves propagating in the dielectric

body 3 and slow transverse waves propagating in the $LiTaO_3$ piezoelectric body 2.

[0051] In the present embodiment, the thickness of the electrode is increased to reduce the acoustic velocity of the SH boundary acoustic waves to less than the acoustic velocities of slow transverse waves propagating in the piezoelectric body 2 and the dielectric body 3. Consequently, the energy of the SH boundary waves concentrates on the boundary between the piezoelectric body 2 and the dielectric body 3. Thus, SH boundary waves with a high electromechanical coupling coefficient k^2 can be propagated with a low propagation loss.

[0052] In addition to the increase in electrode thickness to propagate SH boundary waves, the duty ratio of the strips defining the electrode can be controlled to reduce the acoustic velocity of SH boundary acoustic waves to less than the acoustic velocities of the slow transverse waves propagating in the piezoelectric body 2 and the dielectric body 3, as described below. Thus, the present invention can allow the SH boundary waves to propagate with concentration on the boundary.

[0053] The present invention will be further described in detail with reference to experimental examples.

[Example 1]

[0054] A $LiTaO_3$ substrate with Euler angles of (0°, 90°, 0°), that is a Y-plate X-propagating $LiTaO_3$ substrate, was prepared as the piezoelectric body 2. This $LiTaO_3$ substrate is highly piezoelectric. The dielectric body 3 was formed of SiO_2. SiO_2 is easy to form into a thin layer. The boundary wave device structured according to the present invention propagates boundary waves while distributing part of the vibrational energy in the $LiTaO_3$ substrate and the SiO_2 body. Since the SiO_2 body has a positive frequency temperature coefficient TCF that cancels the negative TCF of the $LiTaO_3$ substrate, the temperature dependence is improved.

[0055] The relationships were examined between the thickness of the electrodes and the acoustic velocity V, electromechanical coupling coefficient k^2, propagation loss α, frequency temperature coefficient TCF, and power flow angle PFA, using electrodes formed of some materials with different densities between the piezoelectric body 2 and the dielectric body 3.

[0056] Figs. 2 to 6, Figs. 7 to 11, and Figs. 12 to 16 show the results of the examination using Au electrodes. Figs. 2 to 6 show the results for SH boundary waves (abbreviated as U2); Figs. 7 to 11 shows the results for Stoneley waves (abbreviated as U3); and Figs. 12 to I6 show the results for longitudinal boundary waves (abbreviated as U1).

[0057] Figs. 17 to 20, Figs. 21 to 24, Figs. 25 to 28, Figs. 29 to 32, Figs. 33 to 36, Figs. 37 to 40, Figs. 41 to 44, and Figs. 45 to 48 show the results of the examination using electrodes formed of Au, Cu, Al, Ag, Fe, Mo, Ni, Pt, Ti, Ta, and W respectively.

[0058] In these figures and the description, U2 represents SH boundary waves, Vm represents an acoustic velocity at a short-circuited boundary, and Vf represents an acoustic velocity at an open boundary. Also, Vs represents an acoustic velocity of slow transverse waves, LT is the abbreviation of $LiTaO_3$, and α represents a propagation loss. For example, Au-U2αm means the propagation loss of SH boundary acoustic waves at a short-circuited boundary with a Au electrode; Au-U2Tm means the frequency temperature coefficient TCF of SH boundary acoustic waves at a short-circuited boundary with a Au electrode; Au-U2Pm means the power flow angle PFA of SH boundary acoustic waves at a short-circuited boundary with a Au electrode.

[0059] The results shown in Figs. 2 to 16 are derived from the calculations in accordance with a document "A method for estimating optimal cuts and propagation directions for excitation and propagation directions for excitation of piezoelectric surface waves" (J. J. Campbell and W. R. Jones, IEEE Trans. Sonics and Ultrason., Vol. SU-15 (1968) pp. 209-217).

[0060] For the open boundary, the acoustic velocity and the propagation loss were calculated assuming that each component of the displacement, the potential, and the electric flux density in the direction of the normal, and the stress in the vertical direction are continuous at each of the boundaries between SiO_2 and Au and between Au and $LiTaO_3$, and that the thicknesses of the SiO_2 and the $LiTaO_3$ are infinity and the Au has a relative dielectric constant of 1. For the short-circuited boundary, the potentials at the boundaries between the SiO_2 and the Au and between the Au and $LiTaO_3$ were assumed to be 0. The electromechanical coupling coefficient k^2 was derived from the following Equation (1):

$$k^2 = 2 \times |Vf - V|/Vf \qquad \text{Equation (1)}$$

where Vf represents acoustic velocity at the open boundary.

[0061] The frequency temperature coefficient TCF was derived from the flowing Equation (2) using phase velocities V at 20°C, 25°C, and 30°C:

$$TCF = V_{(25°C)}^{-1} \times [(V(30°C)-V(20°C))/10°C]-\alpha s$$

Equation (2)

where αS represents the linear expansion coefficient of the $LiTaO_3$ substrate in the propagation direction of boundary waves.

[0062] The power flow angle PFA at Euler angles (ϕ, θ, ψ) was derived from the following Equation (3) using phase velocities V at ψ-0.5°, ψ, and ψ+0.5°:

$$PFA = \tan^{-1}[V_{(\psi)}^{-1} \times (V(\psi + 0.5°) - V(\psi - 0.5°))]$$

Equation (3)

[0063] The acoustic velocities of longitudinal waves, fast transverse waves, and slow transverse waves in the Y-plate X-propagating $LiTaO_3$ are 5589, 4227, and 3351 m/s respectively. The acoustic velocities of longitudinal waves and slow transverse waves in the SiO_2 are 5960 and 3757 m/s respectively.

[0064] As for the acoustic velocity Vm at each short-circuited boundary when the thickness of the Au electrode is 0, Figs. 2 to 16 clearly show that the acoustic velocity of Stoneley waves mainly composed of the U3 wave component is slightly lower than that of slow transverse waves propagating in the $LiTaO_3$ substrate, and that the acoustic velocity of SH boundary acoustic waves mainly composed of the U2 wave component lies between the acoustic velocities of the fast transverse waves and slow transverse waves propagating in the $LiTaO_3$. The K_2 of Stoneley waves is as low as 0 to 0.2%. This means that Stoneley waves are not suitable for RF filters. On the other hand, SH boundary acoustic waves have an electromechanical coupling coefficient k^2 of 3% or more, and are suitably used for the RF filters.

[0065] The longitudinal boundary waves mainly composed of the U1 wave component had so high a propagation loss α that the solution was not able to be obtained, when the Au thickness was 0. It is however considered from the results for the Stoneley waves and the SH boundary acoustic waves that when the Au thickness is 0, the acoustic velocity of the longitudinal boundary waves is slightly lower than that of the longitudinal waves propagating in the $LiTaO_3$ substrate.

[0066] It is shown that the acoustic velocities of the Stoneley waves, the SH boundary acoustic waves, and the longitudinal boundary waves are each reduced when the thickness of the Au electrode is increased.

[0067] In addition, it is shown that when the velocity of the SH boundary acoustic waves is reduced to less than that of the slow transverse waves propagating in the SiO_2, the propagation loss is reduced, and that when the velocity of the SH boundary acoustic waves is further reduced to less than that of the slow transverse waves propagating in the $LiTaO_3$, the propagation loss becomes 0.

[0068] As shown in Figs. 2 to 16, the calculated values became discontinuous under the conditions that the acoustic velocity of the longitudinal waves or the transverse waves was equal to the acoustic velocity of the boundary acoustic waves. This is observed when, for example, the Vm is lower than and the Vf is higher than the velocity of the slow transverse waves propagating in the SiO_2. In other words, this is observed when the conditions for leakage of boundary waves differ between the short-circuited boundary and the open boundary. The calculated values may also be discontinuous because of close acoustic velocities of the SH boundary waves and the Stoneley waves. In particular, calculations for the electromechanical coupling coefficient k^2, for which Vf and Vm are used, often result in discontinuous values.

[0069] Turning now to Figs. 17 to 48, these figures clearly show that when the velocity of the SH boundary waves is reduced to less than that of the slow transverse waves propagating in the SiO_2, the propagation loss is reduced even in use of other metals for the electrode, and that when the velocity of the SH boundary waves is further reduced to less than the slow transverse waves propagating in the $LiTaO_3$, the propagation loss becomes 0.

[0070] Fig. 49 shows the relationship between the thickness H1 of the electrode allowing the acoustic velocity of the SH boundary waves to be reduced to less than that of the slow transverse waves propagating in the SiO_2 and the density ρ of the electrode material, and the relationship between the thickness H2 of the electrode allowing the acoustic velocity of the SH boundary waves to be reduced to less than that of the slow transverse waves propagating in the $LiTaO_3$ and the density ρ of the electrode. As clearly shown in Fig. 49, SH boundary waves with a low propagation loss can be produced by satisfying the following Expression (4), and in particular, SH boundary waves with a propagation loss of 0 can be produced by satisfying Expression (5).

$$H1[\lambda] > 25000\rho^{1.46} \quad (4)$$

$$H2[\lambda] > 1100000\rho^{-1.7} \quad (5)$$

[0071] In the manufacture of this type of boundary acoustic wave device, an electrode, such as IDT is provided on the $LiTaO_3$ piezoelectric substrate by photolithography, such as lift-off or dry etching, and then a dielectric layer of, for example, SiO_2 is formed on the electrode by a thin-layer deposition method, such as a sputtering method, a vapor deposition method, or a CVD method. Consequently, the dielectric layer may grow at a slant angle or nonuniformly to degrade the performance of the resulting boundary acoustic wave device because of the uneven surface resulting from the thickness of the IDT. The thinner the thickness of the electrode the better, from the viewpoint of preventing such degradation.

[0072] A study of the present inventors has found that if an electrode with a thickness H of 0.1λ (λ: wavelength of SH boundary waves) makes it difficult to form a high-quality thin dielectric layer. Also, an electrode with a thickness H of 0.25λ or more results in an aspect ratio of 1 or more. This makes it difficult to form the electrode by inexpensive dry etching or lift-off. Furthermore, the process and apparatus for forming the dielectric layer by a thin-layer deposition method are limited, and generalized RF magnetron sputtering is not suitable for the formation of the dielectric thin layer. The thickness of the electrode is preferably 0.25λ or less, and more preferably 0.1λ or less.

[0073] Fig. 49 suggests that by using a material with the ρ of 2659 kg/m^3 or more for the electrode, the acoustic velocity of SH boundary acoustic waves can be reduced to less than that of transverse waves propagating in the SiO_2 and the thickness H of the electrode can be reduced to 0.25λ or less, the thickness values allowing the decrease of propagation loss. If the material of the electrode has a ρ of 4980 kg/m^3 or more, the thickness H of the electrode can be advantageously reduced to 0.10λ or less, the thickness values allowing the propagation loss to be 0. Thus, the electrode material preferably has a density ρ of 2659 kg/m^3 or more, and more preferably 4980 kg/m^3 or more.

[0074] Furthermore, by using a material with a density ρ of 8089 kg/m^3 or more for the electrode, the electrode thickness H can be reduced to 0.25λ or less, the thickness values allowing the propagation loss of the SH boundary waves to be 0. If the electrode material has a ρ of 13870 kg/m^3 or more, the electrode thickness H can be reduced to 0.10λ or less, the thickness values allowing the propagation loss to be 0 . Thus, the electrode material much preferably has a ρ of 8089 kg/m^3 or more, and most preferably 13870 kg/m^3 or more.

[0075] Figs. 17 to 48 show that by forming the electrode to a thickness satisfying Expression (4), the electromechanical coupling coefficient k^2 is increased to 3% and that the resulting boundary acoustic wave device is suitable as an RF filter.

[0076] In the present invention, the electrode may be in a form of sheet defining a waveguide, a bus bar, and so forth, or may be an IDT or comb-like electrode for exciting the boundary waves, or a reflector for reflecting the boundary waves.

[0077] In the Description, the Euler angles (ϕ, θ, ψ) representing the cutting angle of the cut surface of the substrate and the propagation direction of the boundary waves are based on the right-handed Euler angles described in a document "Acoustic Wave Device Technology Handbook" (in Japanese, Japan Society for the Promotion of Science, Acoustic Wave Device Technology the 150th Committee, 1st Edition 1st printing, published on November 30, 2001, p. 549). Specifically, in LN crystallographic axes X, Y, and Z, the X axis is rotated by ϕ anticlockwise about the Z axis to define an Xa axis. Subsequently, the Z axis is rotated by θ anticlockwise about the Xa axis to define a Z' axis. A plane including the Xa axis and whose normal line is the Z' axis is defined as the cut surface. The propagation direction of the boundary waves is set to be the direction of the X' axis that is defined by rotating the Xa axis by ψ anticlockwise about the Z' axis.

[0078] As for the $LiTaO_3$ crystallographic axes X, Y, and Z defining the initial Euler angles, the Z axis is set to be parallel to the C axis, the X axis is set to be parallel to one of the equivalent a axes extending in three directions, and the Y axis is set to be the normal line of a plane including the X axis and the Z axis.

[0079] Crystallographically equivalent Euler angles suffice for the $LiTaO_3$ Euler angles (ϕ, θ, ψ) in the present invention. For example, Document 7 (Journal of the Acoustical Society of Japan (in Japanese) Vol. 36, No. 3, 1980, pp. 140 to 145) has taught that $LiTaO_3$ belongs to the trigonal 3m point group, and Equation (A) therefore holds.

$$\begin{aligned} F(\phi, \theta, \psi) &= F(60°-\phi, -\theta, \psi) \\ &= F(60°+\phi, -\theta, 180°-\psi) \\ &= F(\phi, 180°+\theta, 180°-\psi) \\ &= F(\phi, \theta, 180°+\psi) \end{aligned} \qquad \text{Equation (A)}$$

where F represents any boundary wave property, such as electromechanical coupling coefficient k^2, propagation loss, TCF, PFA, or a natural unidirectional property. For example, when the propagation direction is reversed, the PFA and the natural unidirectional property are changed in plus/minus sign, but their absolute values do not change; hence they are estimated to be practically equivalent. Although Document 7 has discussed surface waves, the same applies to the

boundary waves in terms of crystalline symmetry. For example, the propagation characteristics of boundary waves with Euler angles of (30°, θ, ψ) are equivalent to those of boundary waves with Euler angles of (90°, 180°-θ, 180°-ψ). For example, the propagation characteristics of boundary waves with Euler angles (30°, 90°, 45°) are equivalent to those of boundary waves with Euler angles shown in Table 1.

[0080] Although the material constants of the electrode used for the calculations in the present invention are those of the electrode in polycrystal, an electrode of a crystal such as an epitaxial film can also provide similar boundary wave propagation characteristics that cause no problem even if the Euler angles are equivalent as expressed by Equation (A). This is because the crystal orientation dependence of the substrate is more dominant for the boundary wave characteristics than that of the film itself.

[Table 1]

ϕ (°)	θ (°)	ψ (°)
30	90	225
30	270	135
30	270	315
90	90	135
90	90	315
90	270	45
90	270	225
150	90	45
150	90	225
150	270	135
150	270	315
210	90	135
210	90	315
210	270	45
210	270	225
270	90	45
270	90	225
270	270	135
270	270	315
330	90	135
330	90	315
330	270	45
330	270	225

[0081] In the present invention, the material of the electrode can be selected not only from the group consisting of Al, Ti, Fe, Cu, Ag, Ta, Au, and Pt, but also from other electroconductive materials. The electrode may include a second electrode layer formed of Ti, Cr, NiCr, or the like on the upper or lower surface of the main electrode layer in order to enhance the adhesion or the electric power resistance. In other words, the electrode may have a multilayer structure.

[0082] The dielectric layer can be formed of not only SiO_2, but also Si, glass, SiN, SiC, ZnO, Ta_2O_5, lead zirconate titanate ceramics, AIN, Al_2O_3, $LiTaO_3$, $LiNbO_3$, An, and so forth. In other words, the dielectric layer may be made of a piezoelectric material. The dielectric layer may have a multilayer structure including a plurality of dielectric layers.

[0083] The boundary acoustic wave device according to the present invention may further include a protective layer outside the structure having the electrode between the $LiTaO_3$ and the dielectric layer. More specifically, the protective layer may be provided on the surface of the dielectric layer opposite the boundary, or the surface of the piezoelectric body opposite the boundary. The protective layer can enhance the strength of the boundary acoustic wave device, or

prevent corrosive gases from infiltrating into the device. The protective layer can be formed of an appropriate material, such as an insulating ceramic, a synthetic resin, or a metal. Synthetic resin protective layers can enhance the resistance to infiltration of corrosive gases and moisture. Insulating ceramic protective layers can enhance the mechanical strength and prevent the infiltration of corrosive gases. Such insulating ceramics include titanium oxide, aluminium nitride, and aluminium oxide. Metal protective layers can enhance the mechanical strength and provide an electromagnetic shielding function. Such metals include Au, Al, and W.

Claims

1. A boundary acoustic wave device comprising a $LiTaO_3$ piezoelectric body, a dielectric body formed on one surface of the piezoelectric body, and an electrode disposed at the boundary between the piezoelectric body and the dielectric body,
wherein the electrode satisfies the expression $H > 1.1 \times 10^6 \rho^{-1.7}$ when the electrode has a density of ρ (kg/m^3) and a thickness of $H(\lambda)$ and boundary acoustic waves have a wavelength of λ.

2. A boundary acoustic wave device comprising a $LiTaO_3$ piezoelectric body, a SiO_2 dielectric body deposited on one surface of the piezoelectric body, and an electrode disposed at the boundary between the piezoelectric body and the dielectric body,
wherein the electrode satisfies the expression $H > 25000\rho^{-1.46}$ when the electrode has a density of ρ (kg/m^3) and a thickness of $H(\lambda)$ and boundary acoustic waves have a wavelength of λ.

3. The boundary acoustic wave device according to Claim 2, wherein the expression $\rho > 2659$ kg/m^3 holds.

4. The boundary acoustic wave device according to Claim 1 or 2, wherein the expression $\rho > 4980$ kg/m^3 holds.

5. The boundary acoustic wave device according to any one of Claims 1 to 4,
wherein the electrode mainly comprises an electrode layer made of at least one metal selected from the group consisting of Al, Ti, Fe, Cu, Ag, Ta, Au, and Pt.

6. The boundary acoustic wave device according to Claim 5, wherein the electrode further comprises a second electrode layer provided on the upper or lower surface of the electrode layer and made of a different electrode material from the electrode layer.

7. The boundary acoustic wave device according to any one of Claims 1 and 4 to 6, wherein the dielectric body is made of a non-piezoelectric material.

8. The boundary acoustic wave device according to any one of Claims 1 to 7, wherein the dielectric body has a multilayer structure including a plurality of dielectric layers.

9. The boundary acoustic wave device according to any one of Claims 1 and 4 to 6, wherein the dielectric layer is made of at least one selected from the group consisting of Si, SiO_2, glass, SiN, SiC, ZnO, Ta_2O_5, lead zirconate titanate ceramics, AlN, Al_2O_3, $LiTaO_3$, $LiNbO_3$, and potassium niobate (KN).

10. The boundary acoustic wave device according to any one of Claims 1 to 9, wherein the dielectric layer is formed by a deposition method.

11. The boundary acoustic wave device according to any one of Claims 1 to 10, further comprising a resin layer formed on the surface of the dielectric layer opposite the boundary.

FIG.1

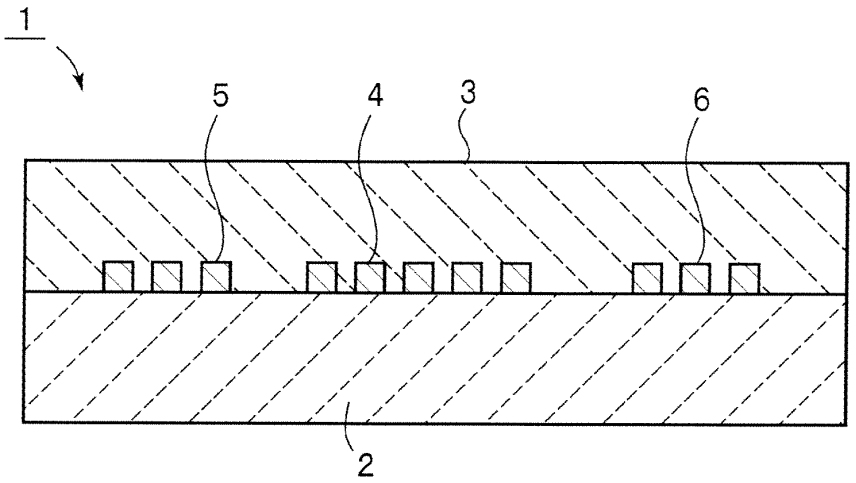
1
5
4
3
6
2

FIG.2

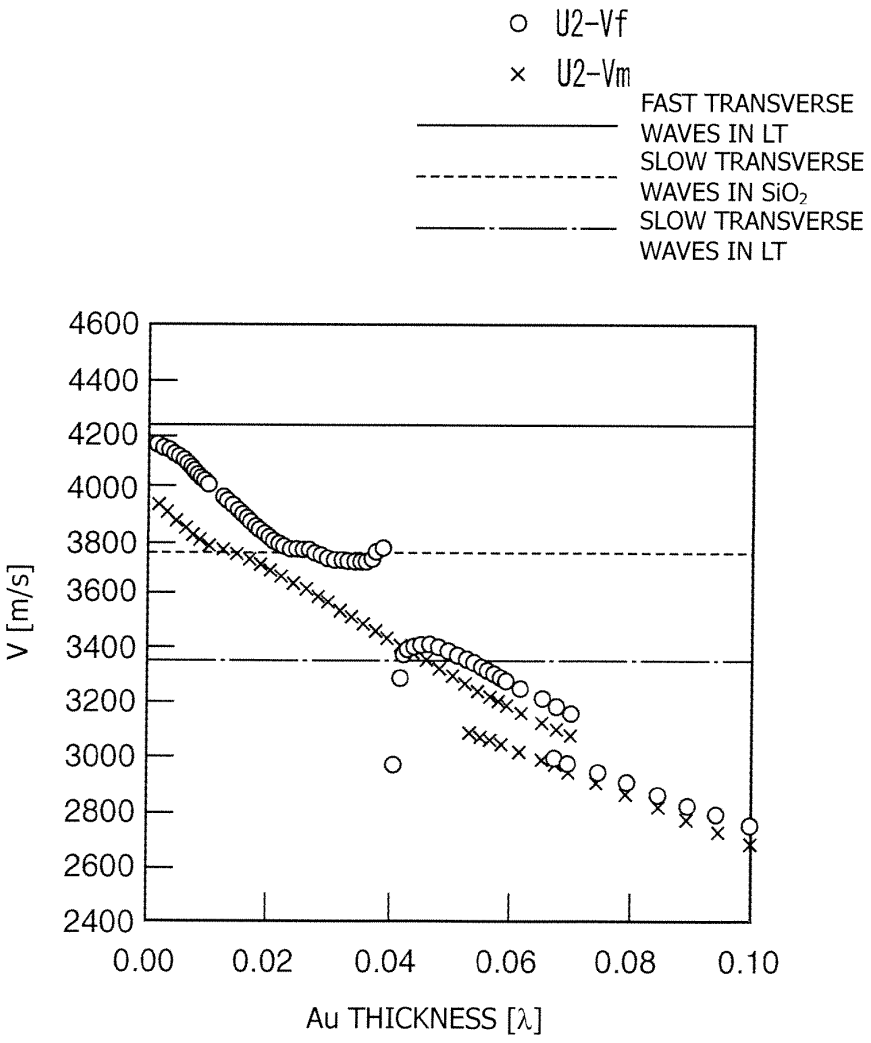
U2-Vf
U2-Vm
FAST TRANSVERSE WAVES IN LT
SLOW TRANSVERSE WAVES IN SiO_2
SLOW TRANSVERSE WAVES IN LT
V [m/s]
4600
4400
4200
4000
3800
3600
3400
3200
3000
2800
2600
2400
0.00
0.02
0.04
0.06
0.08
0.10
Au THICKNESS [λ]

FIG.3

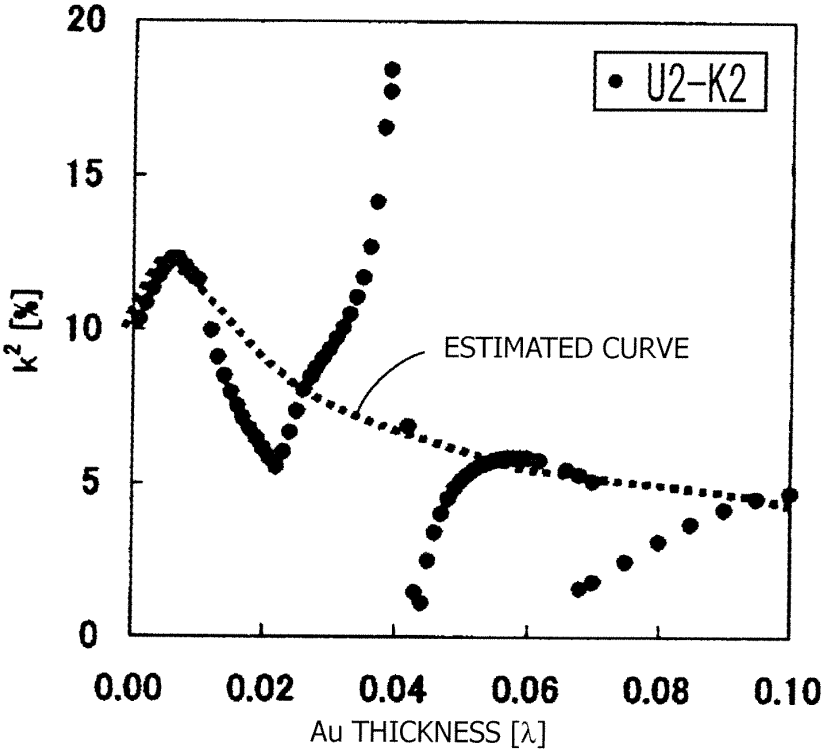
20
15
10
5
0
k^2 [%]
U2-K2
ESTIMATED CURVE
0.00
0.02
0.04
0.06
0.08
0.10
Au THICKNESS [λ]

FIG.4

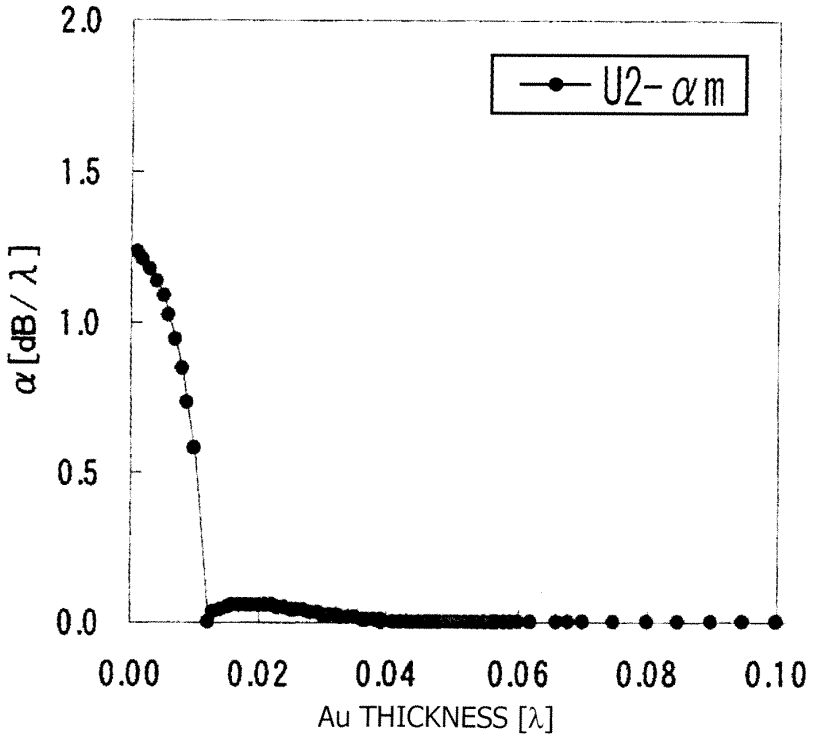
2.0
1.5
1.0
0.5
0.0
α [dB/λ]
U2-αm
0.00
0.02
0.04
0.06
0.08
0.10
Au THICKNESS [λ]

FIG.5

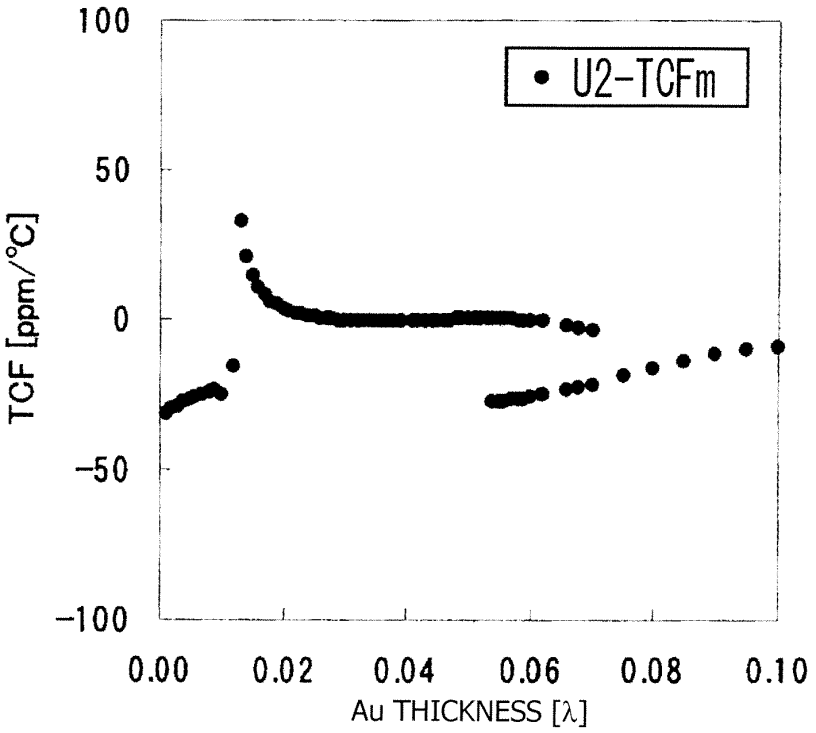
100
50
0
−50
−100
TCF [ppm/°C]
U2-TCFm
0.00
0.02
0.04
0.06
0.08
0.10
Au THICKNESS [λ]

FIG.6

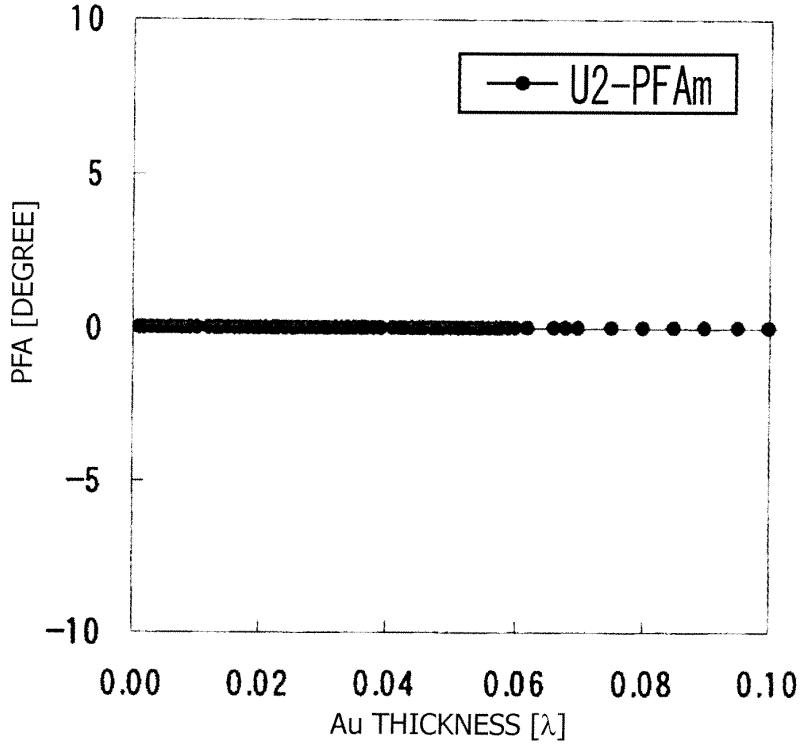
10
5
0
−5
−10
PFA [DEGREE]
U2-PFAm
0.00
0.02
0.04
0.06
0.08
0.10
Au THICKNESS [λ]

FIG.7

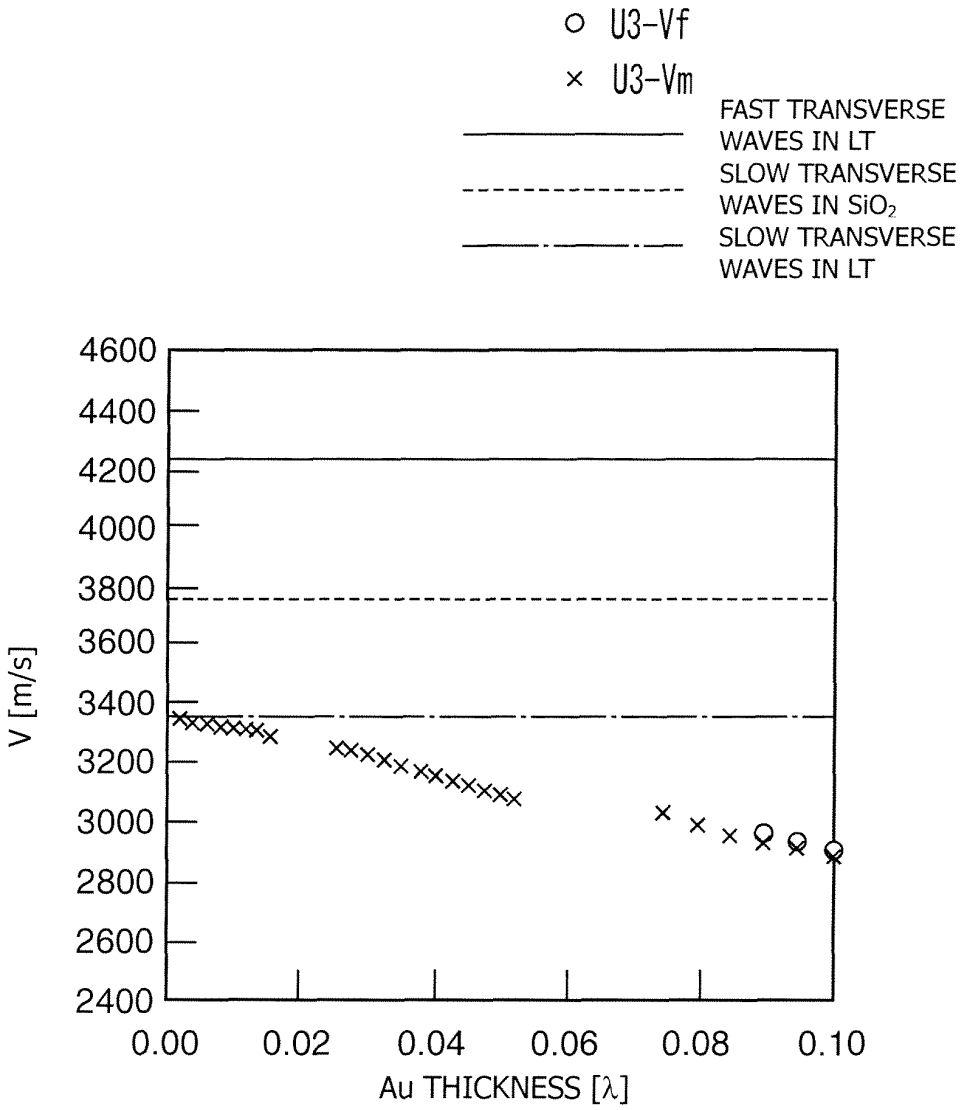
○ U3-Vf
× U3-Vm
FAST TRANSVERSE WAVES IN LT
SLOW TRANSVERSE WAVES IN SiO2
SLOW TRANSVERSE WAVES IN LT
V [m/s]
4600
4400
4200
4000
3800
3600
3400
3200
3000
2800
2600
2400
0.00
0.02
0.04
0.06
0.08
0.10
Au THICKNESS [λ]

FIG.8

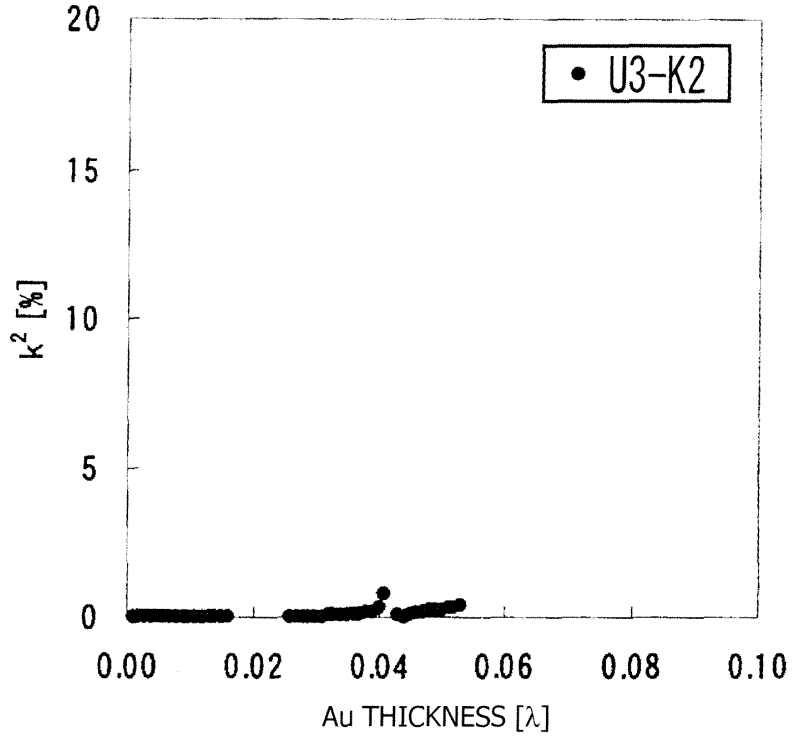
20
15
10
5
0
k^2 [%]
• U3-K2
0.00
0.02
0.04
0.06
0.08
0.10
Au THICKNESS [λ]

FIG.9

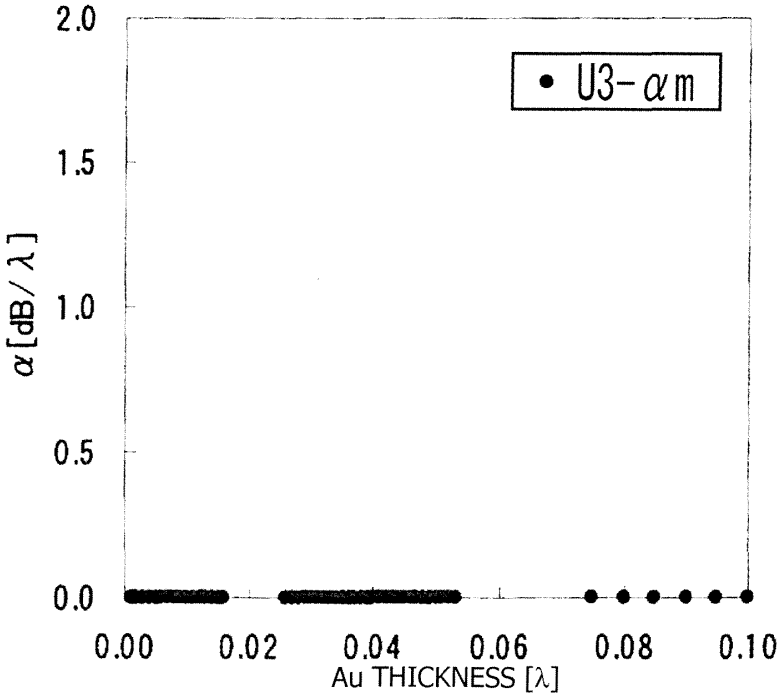
2.0
1.5
1.0
0.5
0.0
α[dB/λ]
• U3-αm
0.00
0.02
0.04
0.06
0.08
0.10
Au THICKNESS [λ]

FIG.10

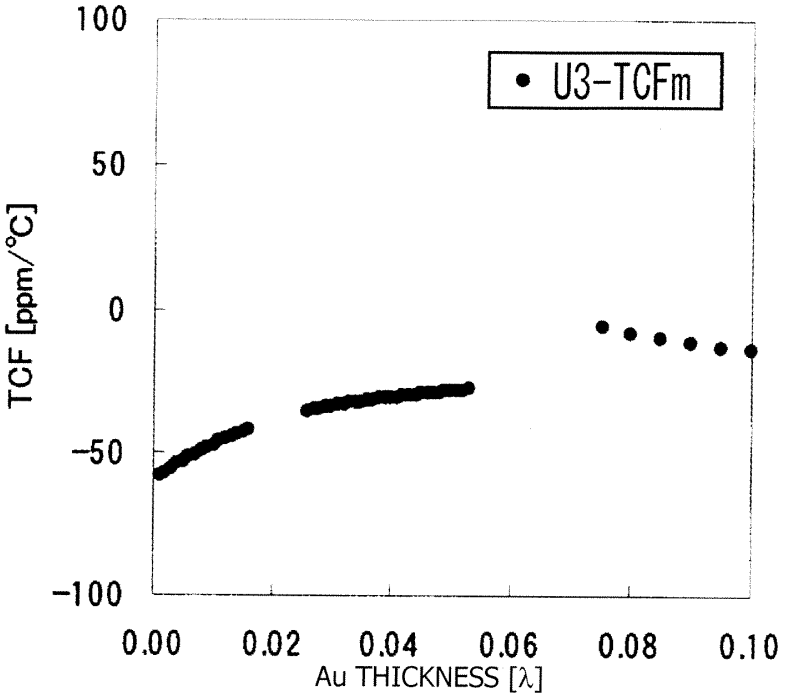
U3-TCFm
TCF [ppm/°C]
100
50
0
−50
−100
0.00
0.02
0.04
0.06
0.08
0.10
Au THICKNESS [λ]

FIG.11

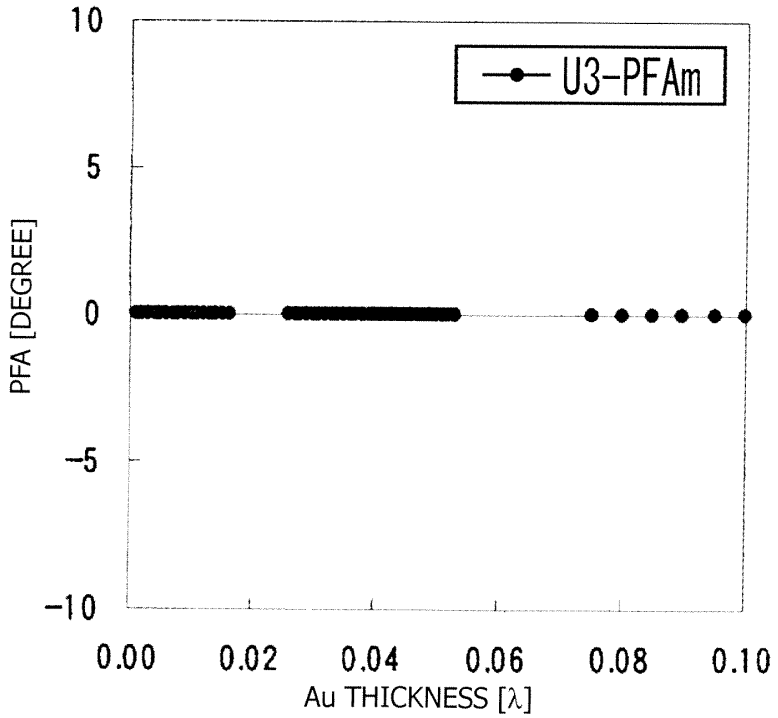
U3-PFAm
PFA [DEGREE]
10
5
0
−5
−10
0.00
0.02
0.04
0.06
0.08
0.10
Au THICKNESS [λ]

FIG.12

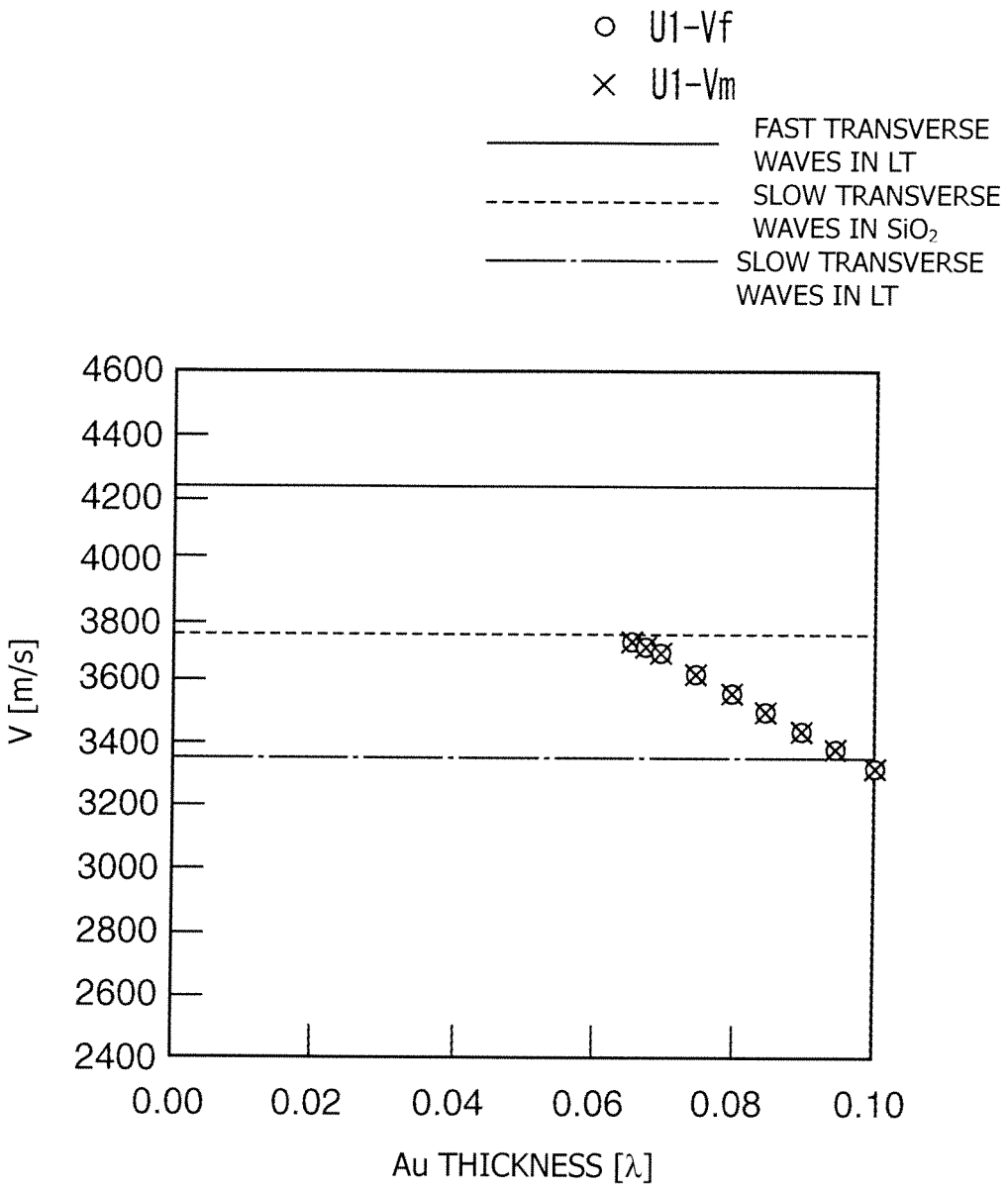
U1-Vf
U1-Vm
FAST TRANSVERSE WAVES IN LT
SLOW TRANSVERSE WAVES IN SiO_2
SLOW TRANSVERSE WAVES IN LT
V [m/s]
4600
4400
4200
4000
3800
3600
3400
3200
3000
2800
2600
2400
0.00
0.02
0.04
0.06
0.08
0.10
Au THICKNESS [λ]

FIG.13

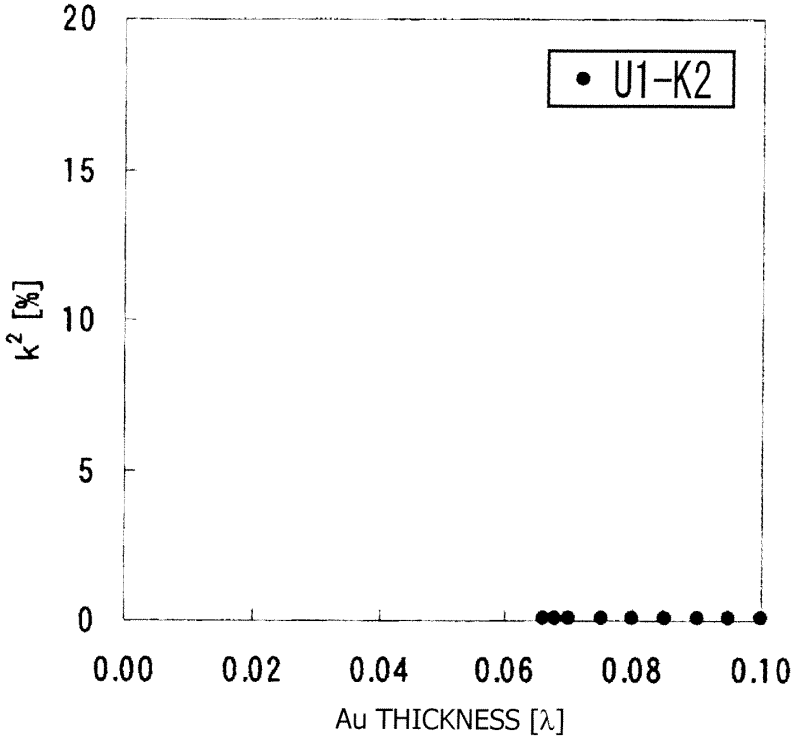
20
15
10
5
0
k^2 [%]
• U1-K2
0.00
0.02
0.04
0.06
0.08
0.10
Au THICKNESS [λ]

FIG.14

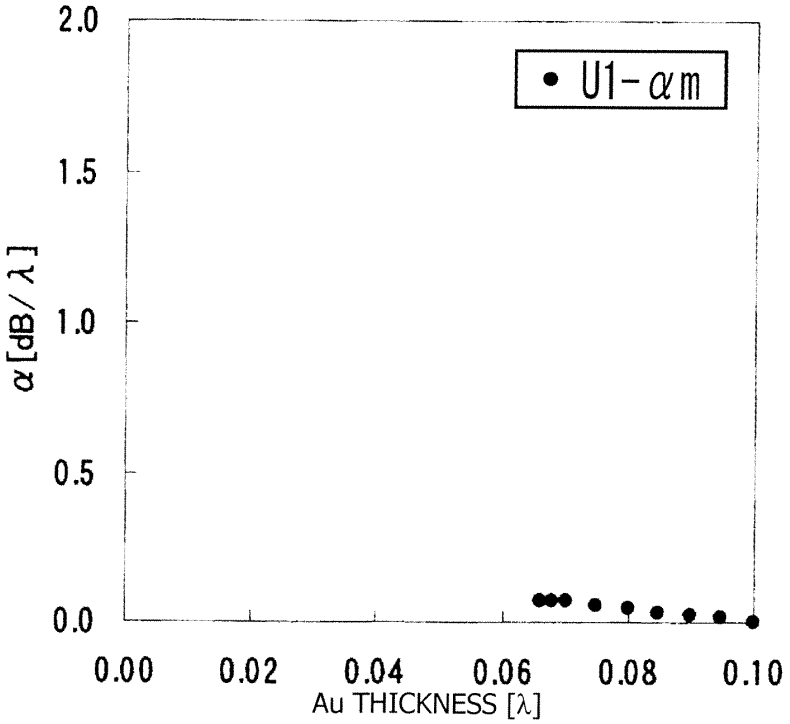
2.0
1.5
1.0
0.5
0.0
α [dB/λ]
• U1-αm
0.00
0.02
0.04
0.06
0.08
0.10
Au THICKNESS [λ]

FIG.15

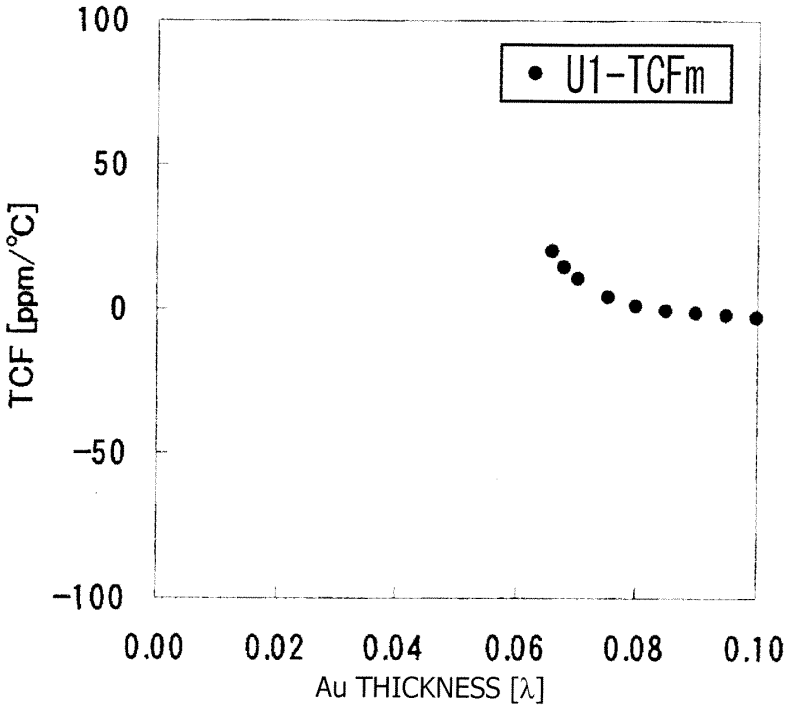
100
50
0
−50
−100
TCF [ppm/°C]
U1-TCFm
0.00
0.02
0.04
0.06
0.08
0.10
Au THICKNESS [λ]

FIG.16

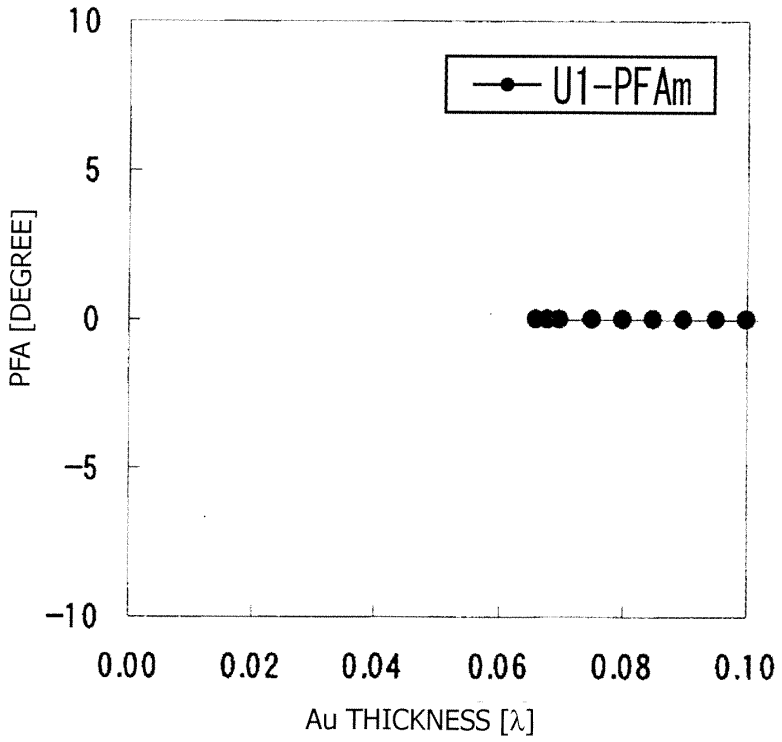
10
5
0
−5
−10
PFA [DEGREE]
U1-PFAm
0.00
0.02
0.04
0.06
0.08
0.10
Au THICKNESS [λ]

FIG.17

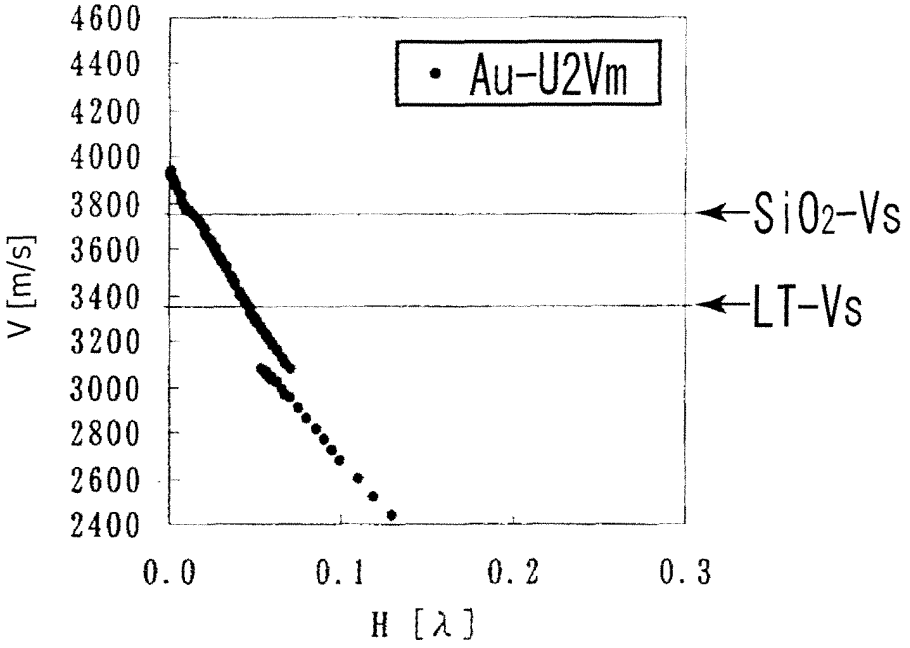
4600
4400
4200
4000
3800
3600
3400
3200
3000
2800
2600
2400
V [m/s]
• Au-U2Vm
←SiO2-Vs
←LT-Vs
0.0
0.1
0.2
0.3
H [λ]

FIG.18

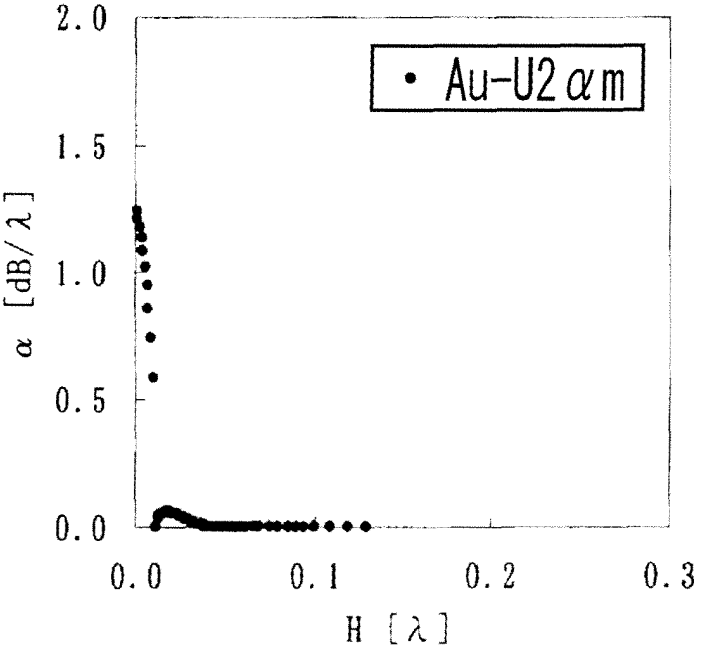
2.0
1.5
1.0
0.5
0.0
α [dB/λ]
• Au-U2αm
0.0
0.1
0.2
0.3
H [λ]

FIG.19

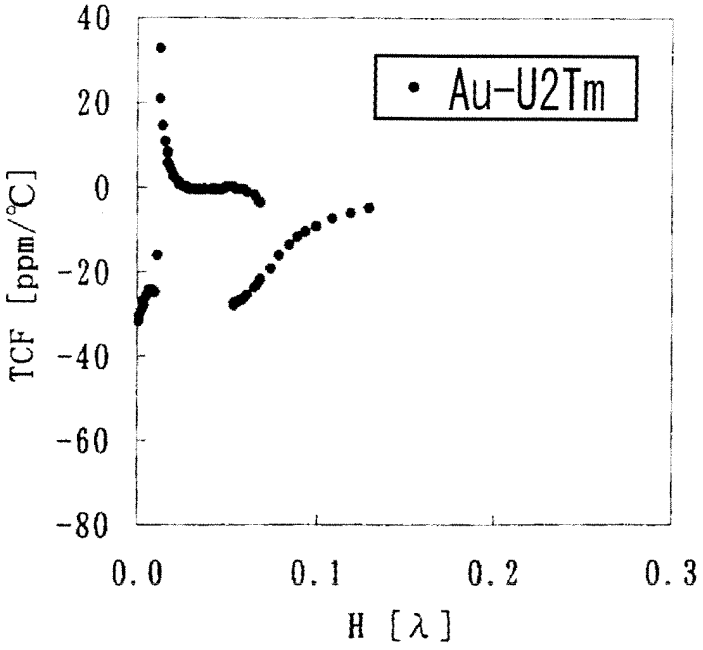
40
20
0
-20
-40
-60
-80
TCF [ppm/°C]
• Au-U2Tm
0.0
0.1
0.2
0.3
H [λ]

FIG.20

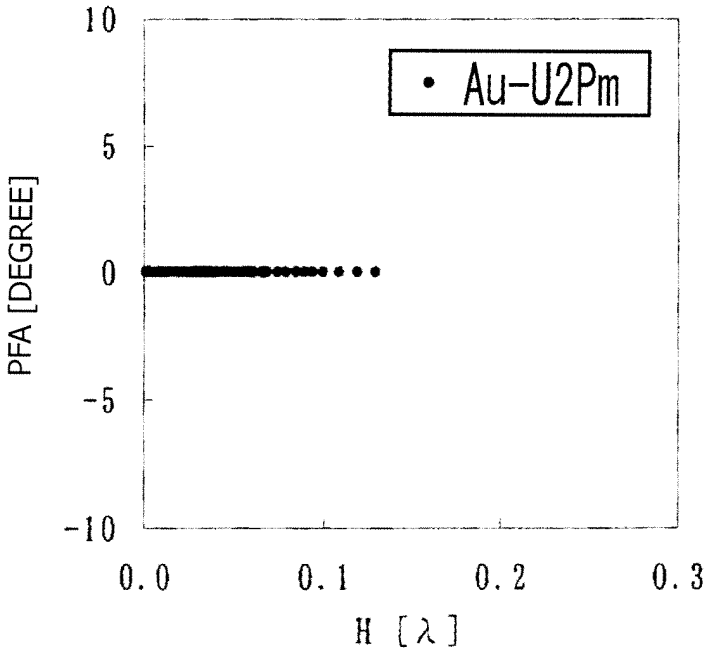
10
5
0
-5
-10
PFA [DEGREE]
• Au-U2Pm
0.0
0.1
0.2
0.3
H [λ]

FIG.21

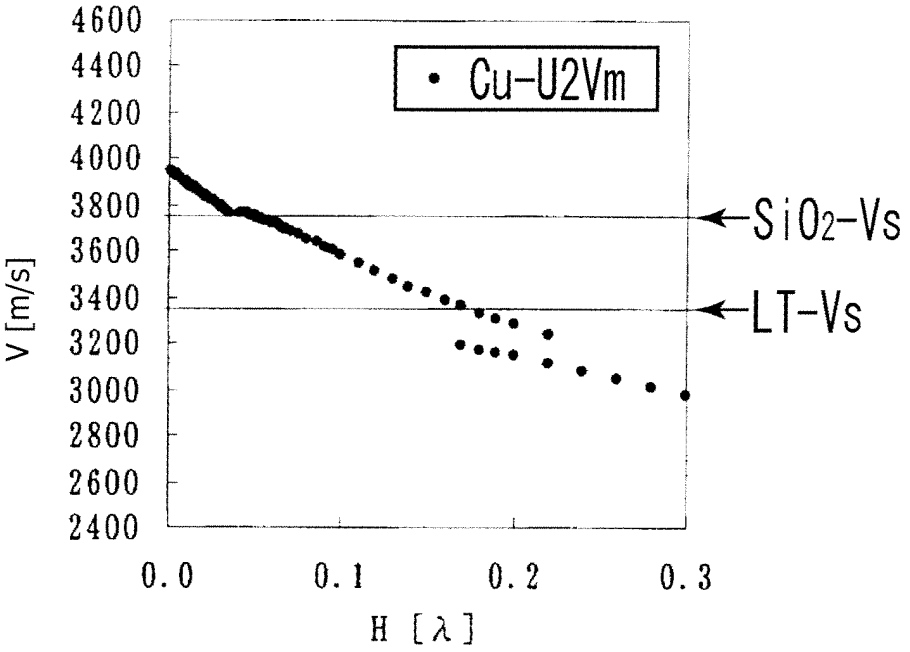
4600
4400
4200
4000
3800
3600
3400
3200
3000
2800
2600
2400
V [m/s]
• Cu-U2Vm
SiO2-Vs
LT-Vs
0.0
0.1
0.2
0.3
H [λ]

FIG.22

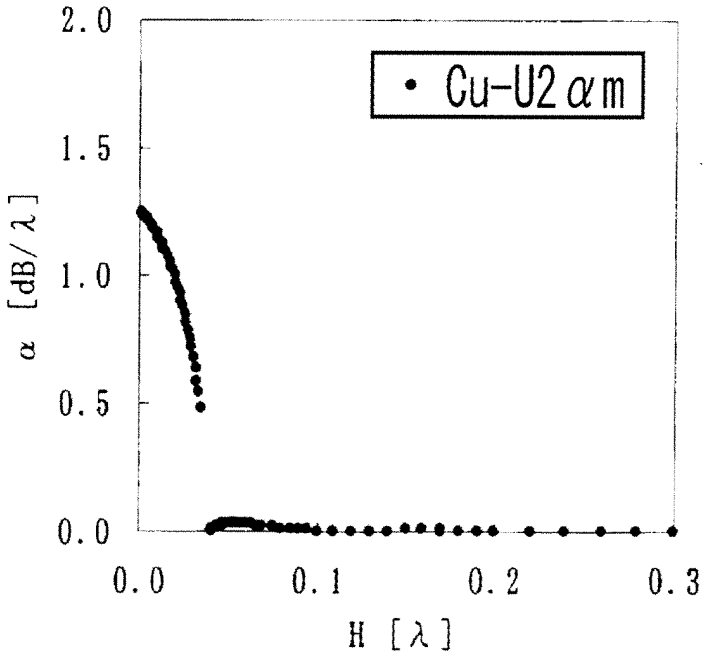
2.0
1.5
1.0
0.5
0.0
α [dB/λ]
• Cu-U2αm
0.0
0.1
0.2
0.3
H [λ]

FIG.23

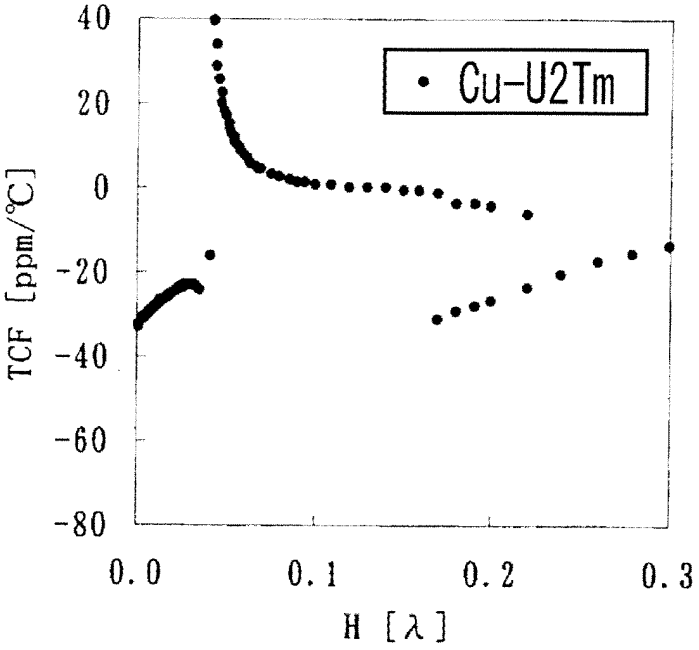
40
20
0
-20
-40
-60
-80
TCF [ppm/℃]
0.0
0.1
0.2
0.3
H [λ]
Cu-U2Tm

FIG.24

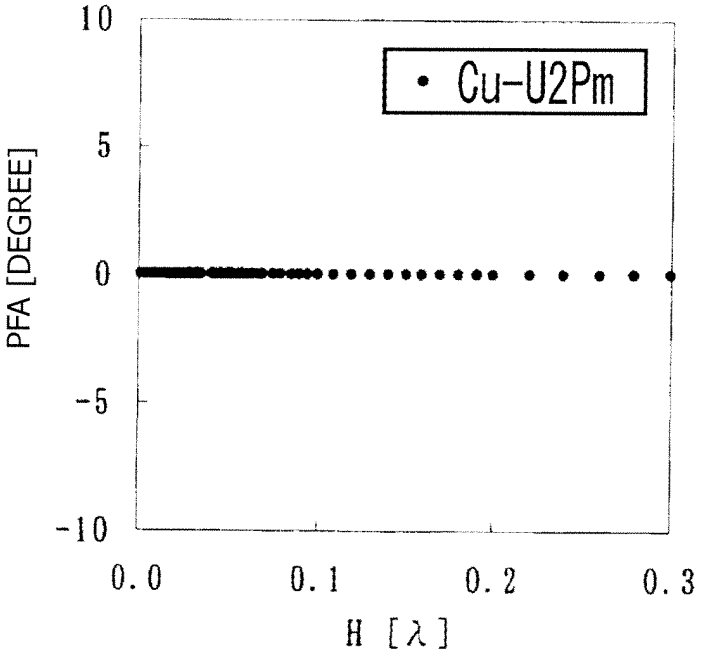
10
5
0
-5
-10
PFA [DEGREE]
0.0
0.1
0.2
0.3
H [λ]
Cu-U2Pm

FIG.25

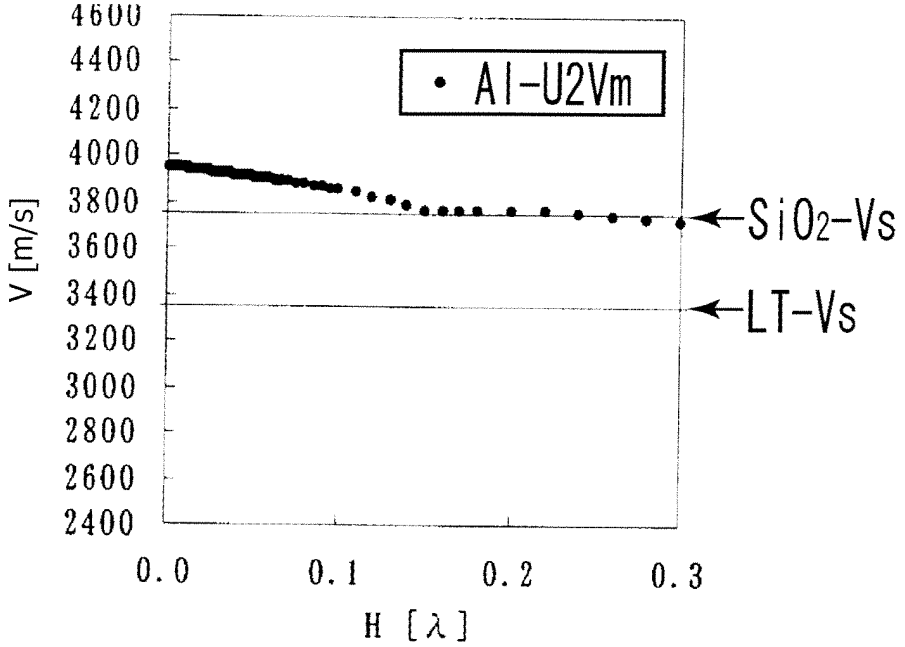
4600
4400
4200
4000
3800
3600
3400
3200
3000
2800
2600
2400
V [m/s]
• Al-U2Vm
SiO2-Vs
LT-Vs
0.0
0.1
0.2
0.3
H [λ]

FIG.26

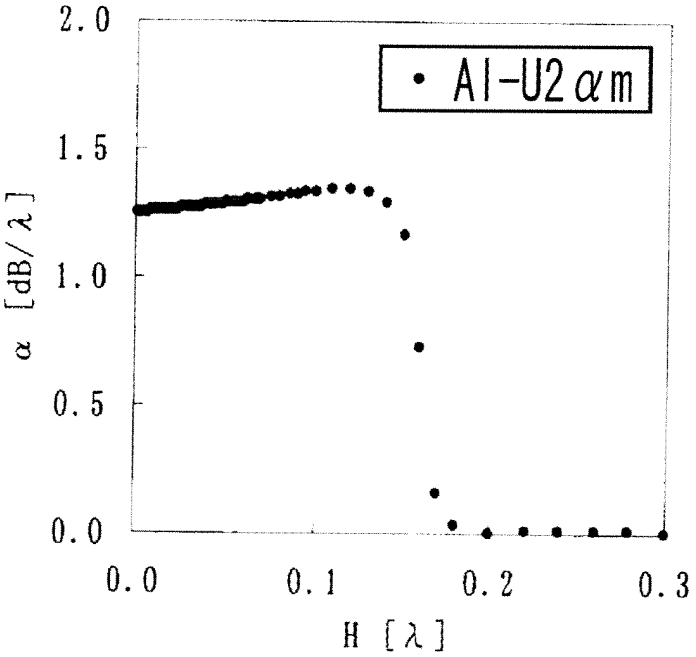
2.0
1.5
1.0
0.5
0.0
α [dB/λ]
• Al-U2αm
0.0
0.1
0.2
0.3
H [λ]

FIG.27

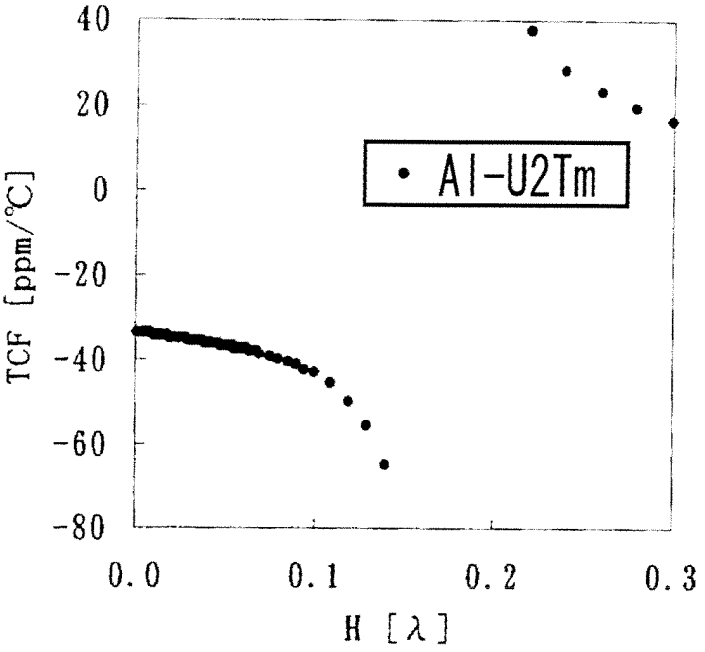
40
20
0
-20
-40
-60
-80
TCF [ppm/℃]
• Al-U2Tm
0.0
0.1
0.2
0.3
H [λ]

FIG.28

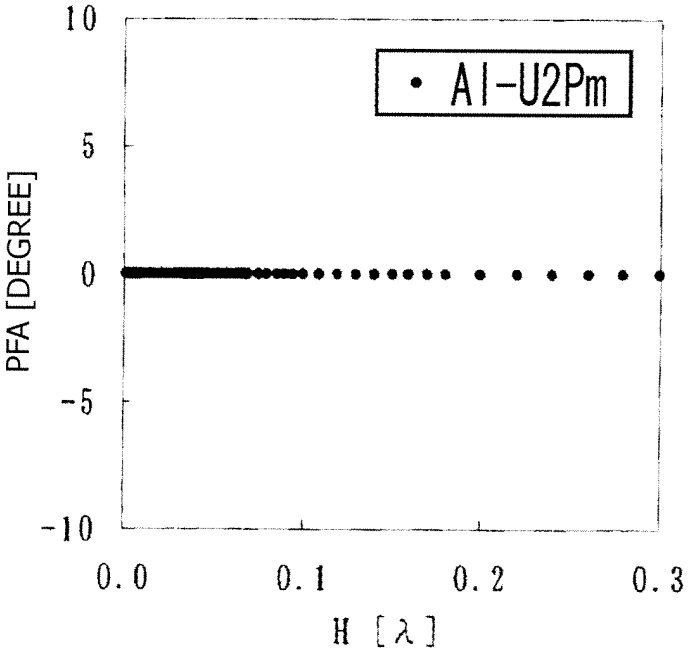
10
5
0
-5
-10
PFA [DEGREE]
• Al-U2Pm
0.0
0.1
0.2
0.3
H [λ]

FIG.29

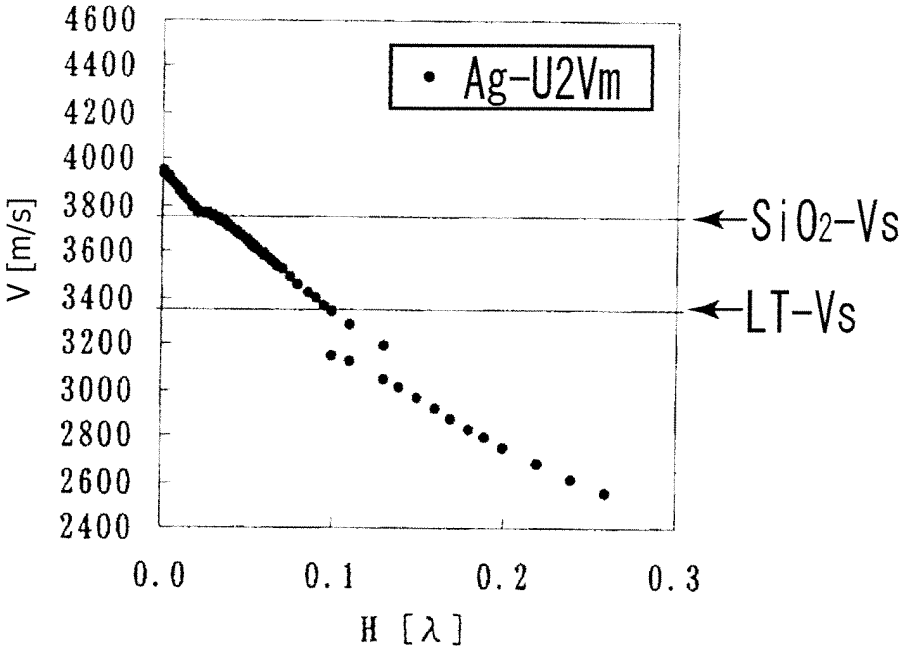
4600
4400
4200
4000
3800
3600
3400
3200
3000
2800
2600
2400
V [m/s]
• Ag-U2Vm
←SiO2-Vs
←LT-Vs
0.0
0.1
0.2
0.3
H [λ]

FIG.30

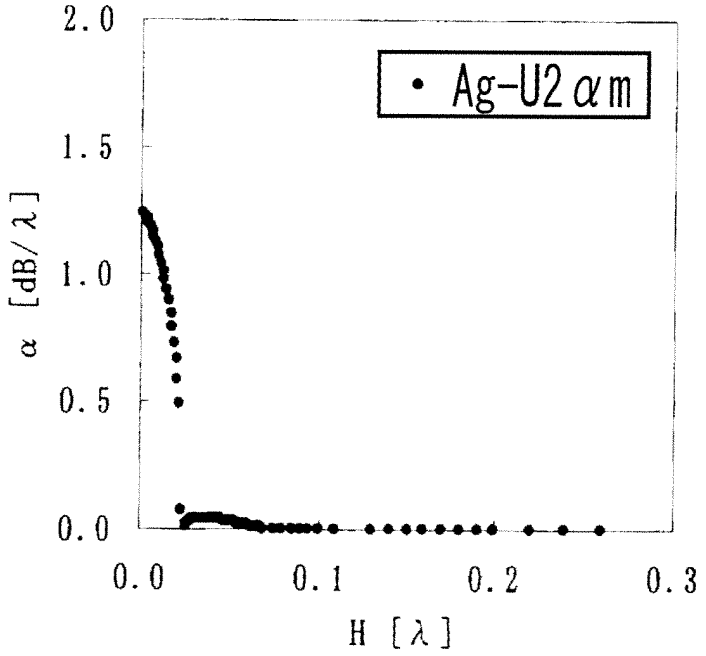
2.0
1.5
1.0
0.5
0.0
α [dB/λ]
• Ag-U2αm
0.0
0.1
0.2
0.3
H [λ]

FIG.31

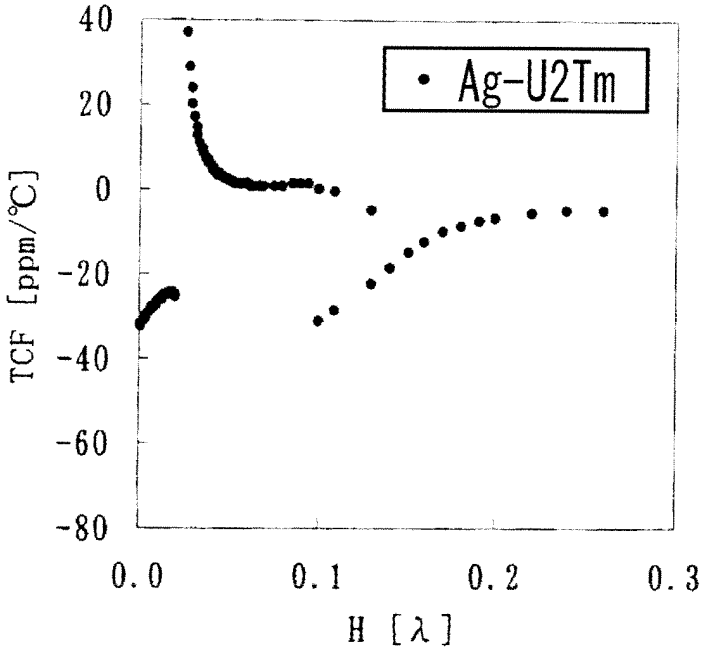
40
20
0
-20
-40
-60
-80
TCF [ppm/℃]
0.0
0.1
0.2
0.3
H [λ]
Ag-U2Tm

FIG.32

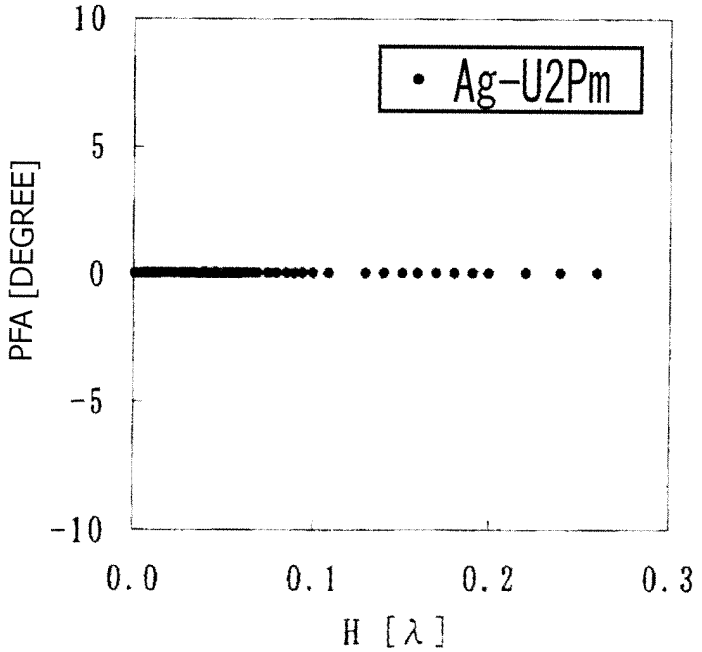
10
5
0
-5
-10
PFA [DEGREE]
0.0
0.1
0.2
0.3
H [λ]
Ag-U2Pm

FIG.33

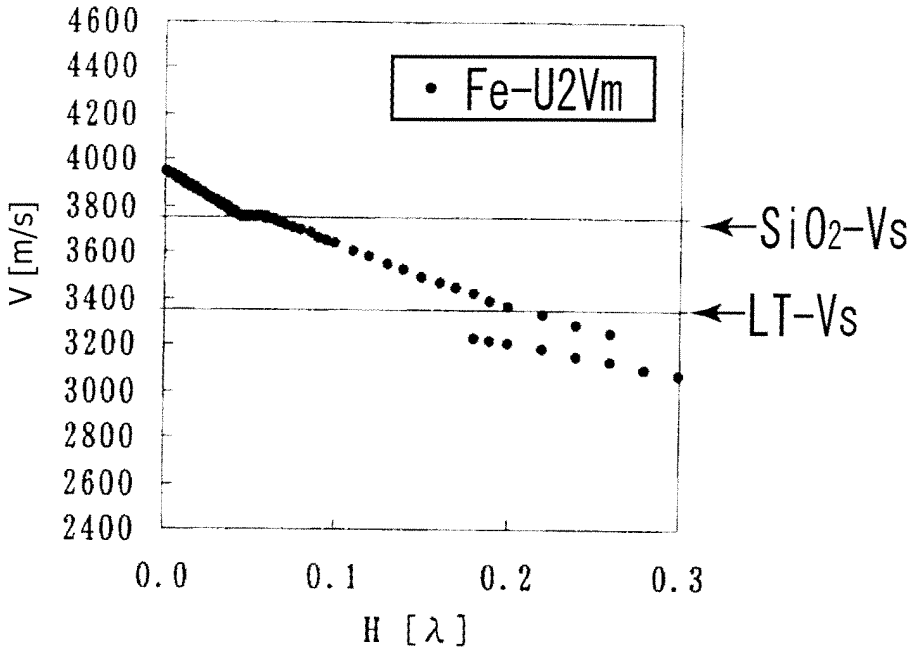
4600
4400
4200
4000
3800
3600
3400
3200
3000
2800
2600
2400
V [m/s]
• Fe-U2Vm
SiO2-Vs
LT-Vs
0.0
0.1
0.2
0.3
H [λ]

FIG.34

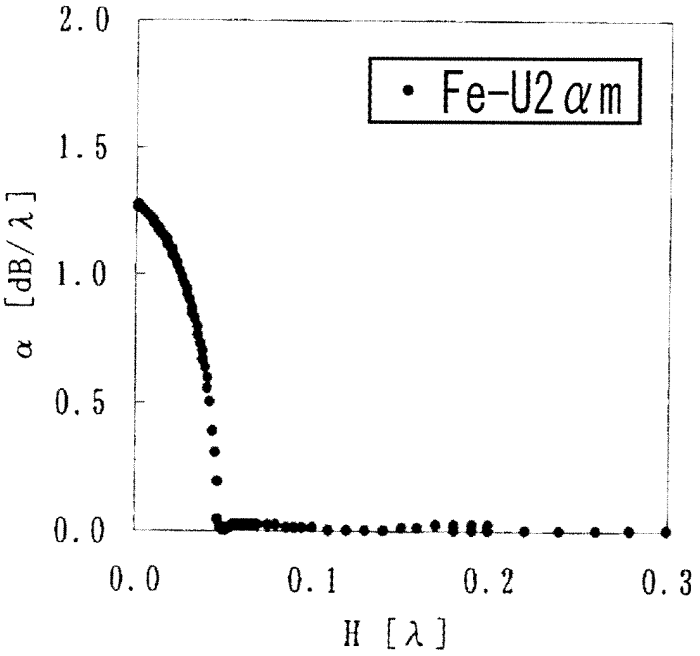
2.0
1.5
1.0
0.5
0.0
α [dB/λ]
• Fe-U2αm
0.0
0.1
0.2
0.3
H [λ]

FIG.35

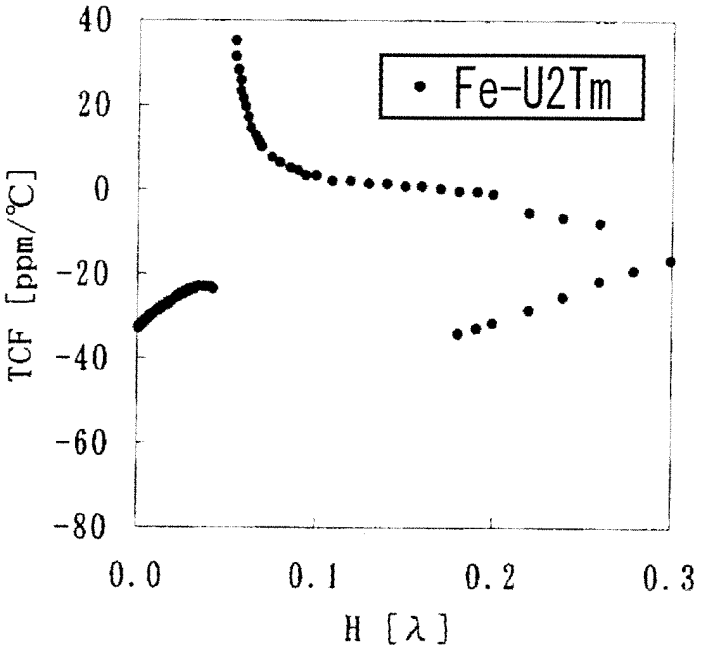
40
20
0
-20
-40
-60
-80
TCF [ppm/℃]
0.0
0.1
0.2
0.3
H [λ]
• Fe-U2Tm

FIG.36

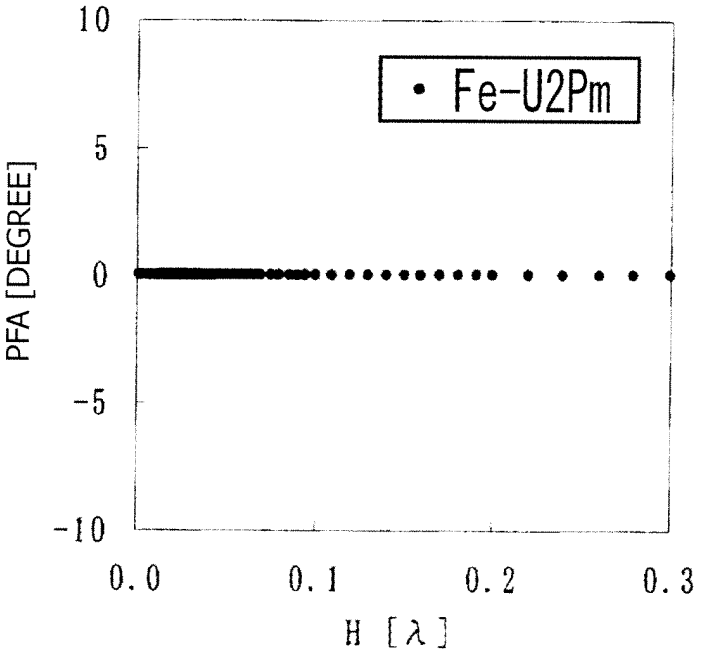
10
5
0
-5
-10
PFA [DEGREE]
0.0
0.1
0.2
0.3
H [λ]
• Fe-U2Pm

FIG.37

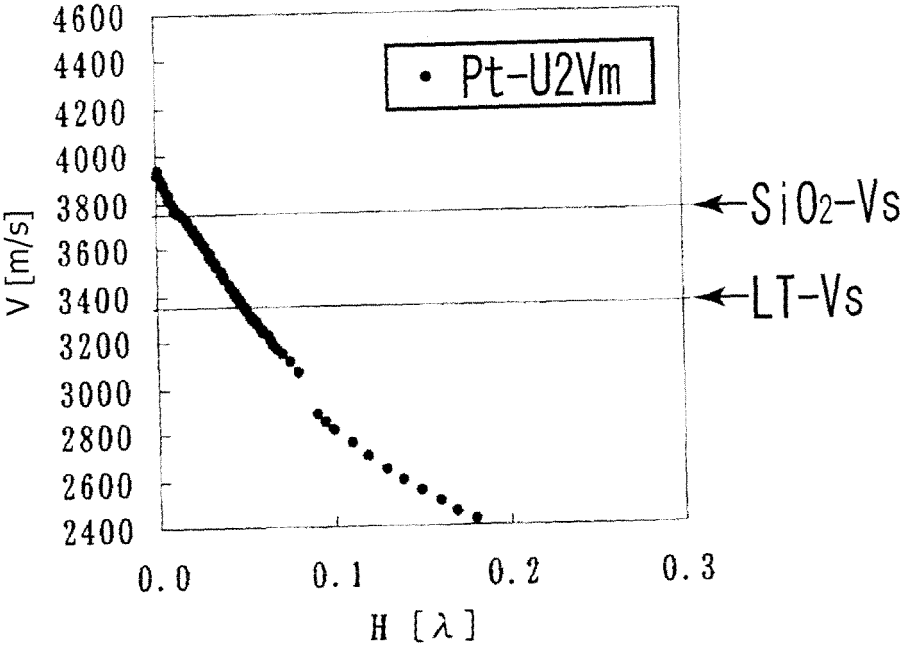
4600
4400
4200
4000
3800
3600
3400
3200
3000
2800
2600
2400
V [m/s]
• Pt-U2Vm
←SiO2-Vs
←LT-Vs
0.0
0.1
0.2
0.3
H [λ]

FIG.38

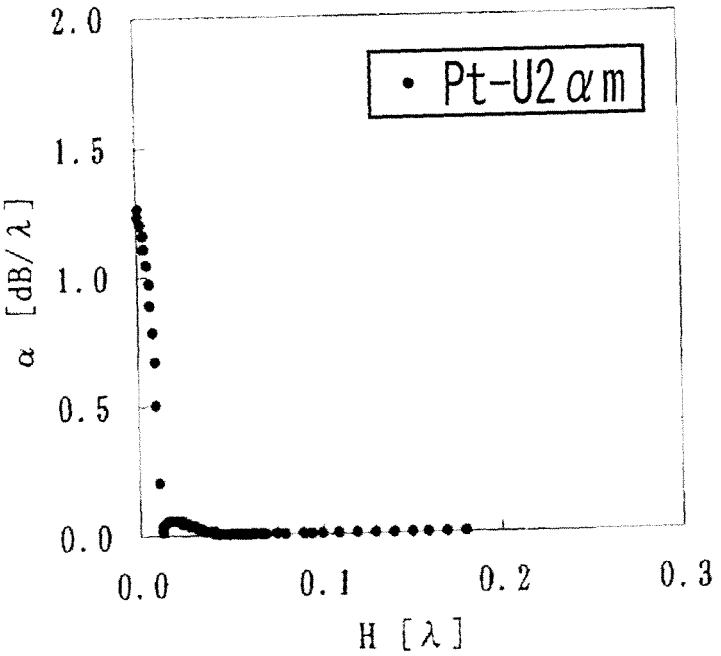
2.0
1.5
1.0
0.5
0.0
α [dB/λ]
• Pt-U2αm
0.0
0.1
0.2
0.3
H [λ]

FIG.39

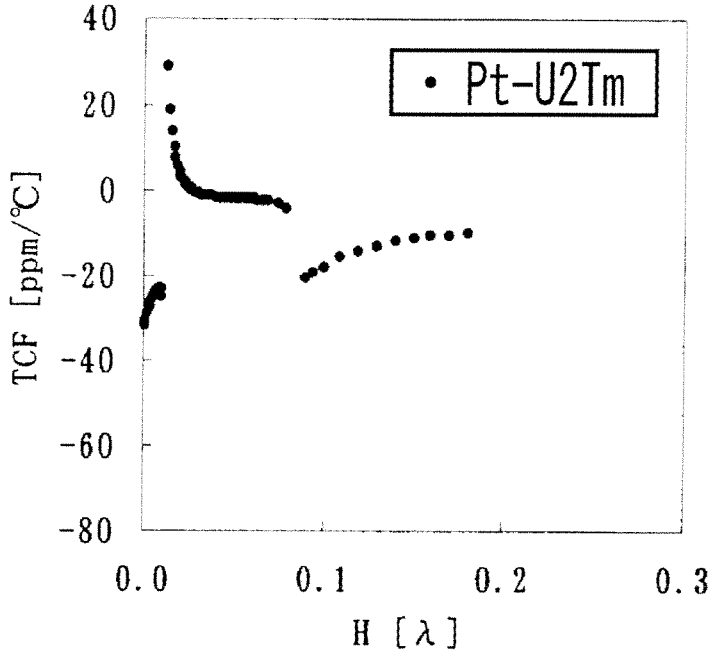
40
20
0
-20
-40
-60
-80
TCF [ppm/℃]
0.0
0.1
0.2
0.3
H [λ]
• Pt-U2Tm

FIG.40

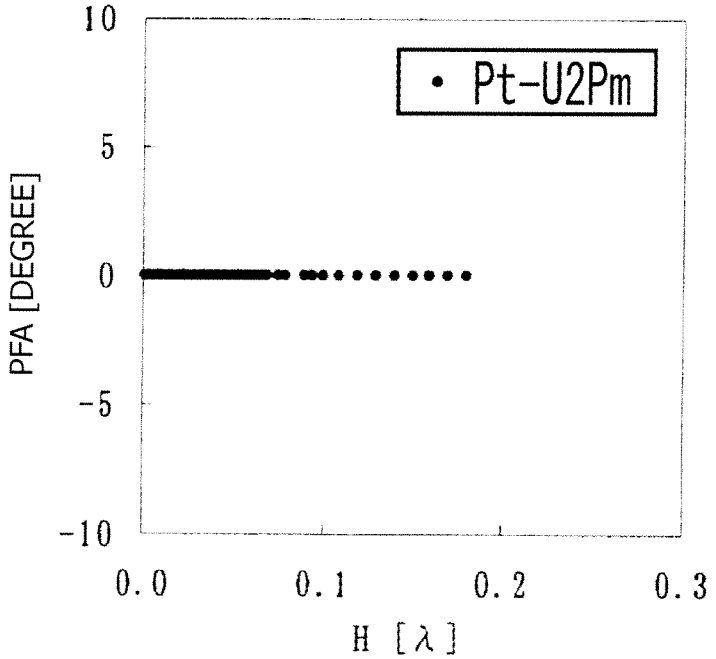
10
5
0
-5
-10
PFA [DEGREE]
0.0
0.1
0.2
0.3
H [λ]
• Pt-U2Pm

FIG.41

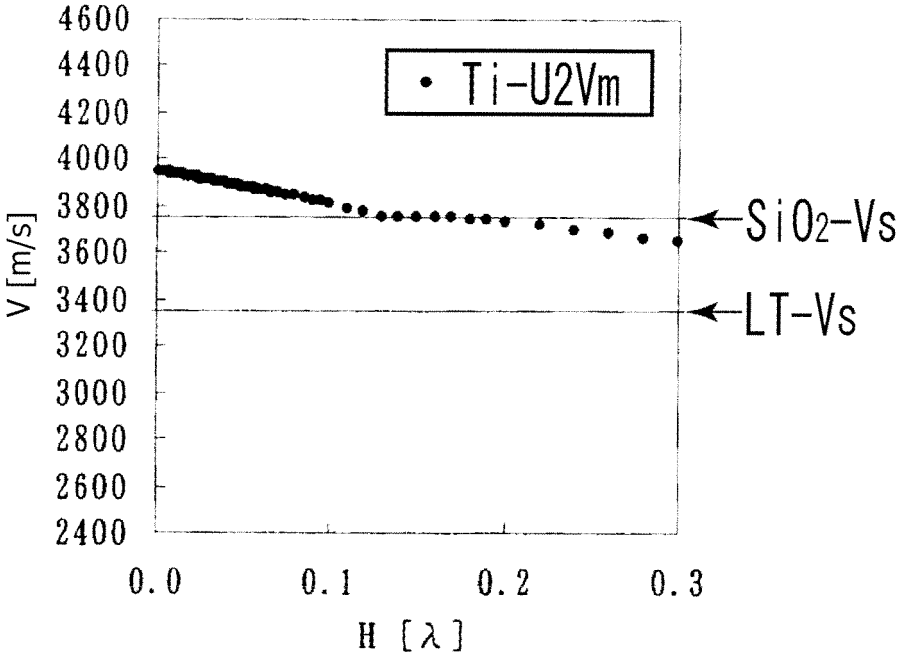
4600
4400
4200
4000
3800
3600
3400
3200
3000
2800
2600
2400
V [m/s]
• Ti-U2Vm
SiO2-Vs
LT-Vs
0.0
0.1
0.2
0.3
H [λ]

FIG.42

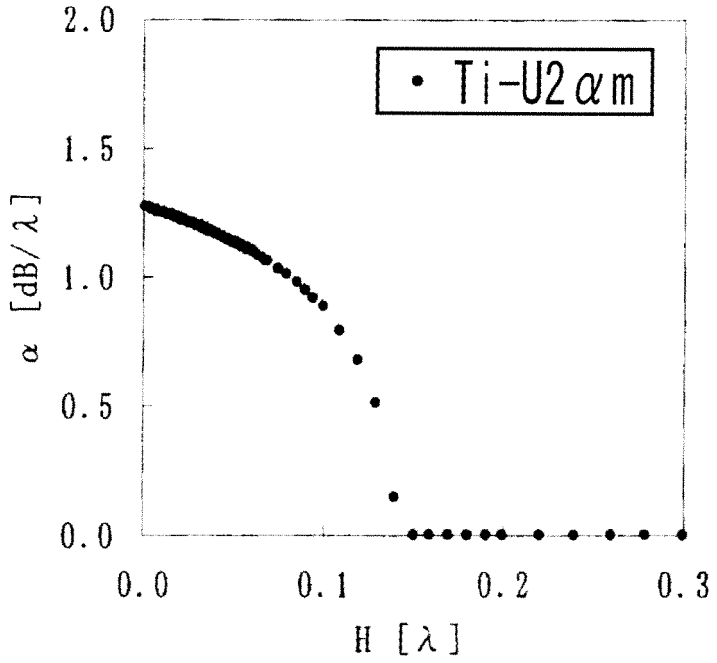
2.0
1.5
1.0
0.5
0.0
α [dB/λ]
• Ti-U2αm
0.0
0.1
0.2
0.3
H [λ]

FIG.43

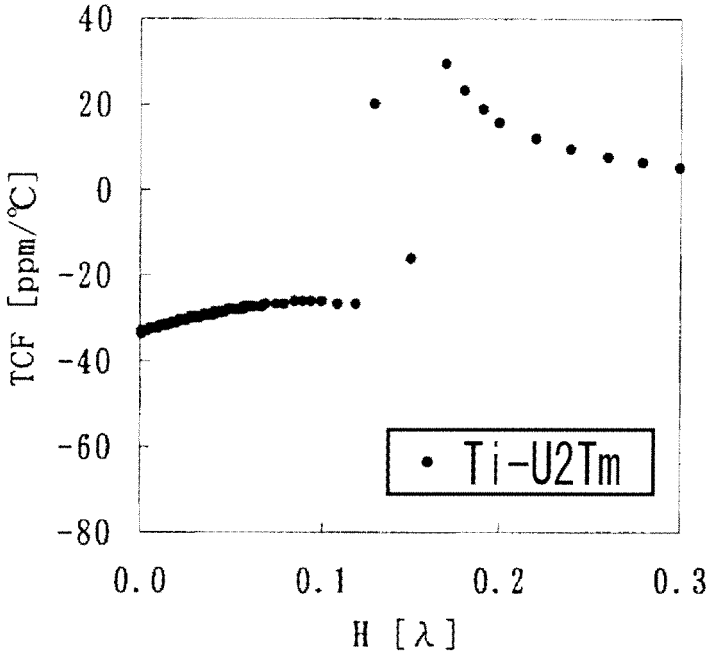
40
20
0
-20
-40
-60
-80
TCF [ppm/℃]
0.0
0.1
0.2
0.3
H [λ]
Ti-U2Tm

FIG.44

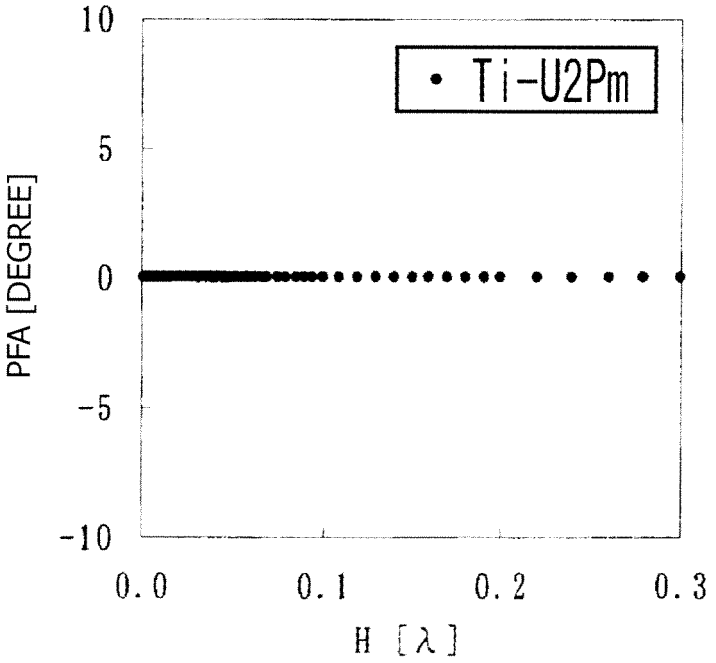
10
5
0
-5
-10
PFA [DEGREE]
0.0
0.1
0.2
0.3
H [λ]
Ti-U2Pm

FIG.45

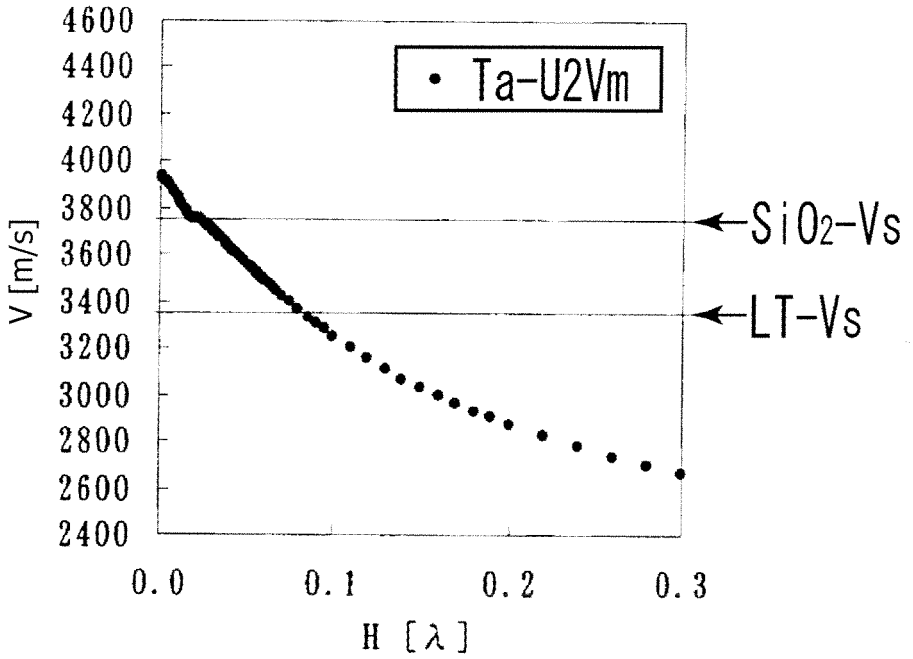
4600
4400
4200
4000
3800
3600
3400
3200
3000
2800
2600
2400
V [m/s]
• Ta-U2Vm
SiO2-Vs
LT-Vs
0.0
0.1
0.2
0.3
H [λ]

FIG.46

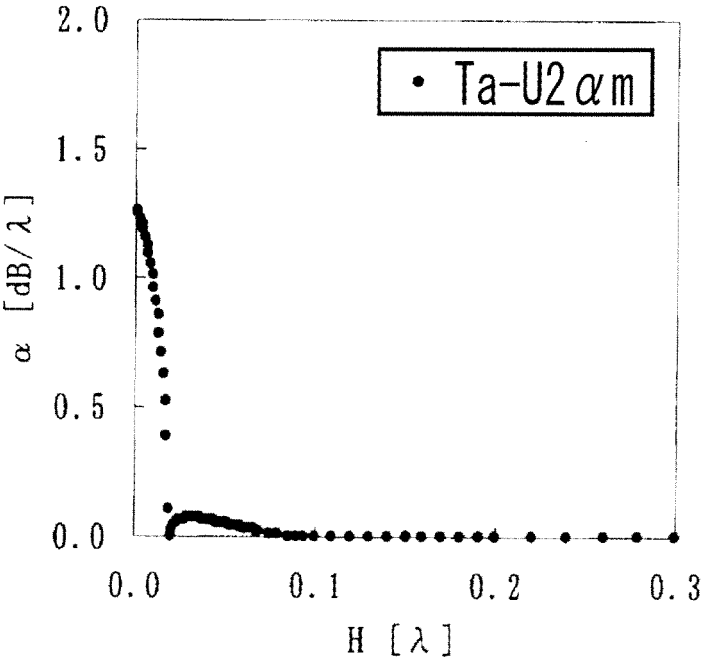
2.0
1.5
1.0
0.5
0.0
α [dB/λ]
• Ta-U2αm
0.0
0.1
0.2
0.3
H [λ]

FIG.47

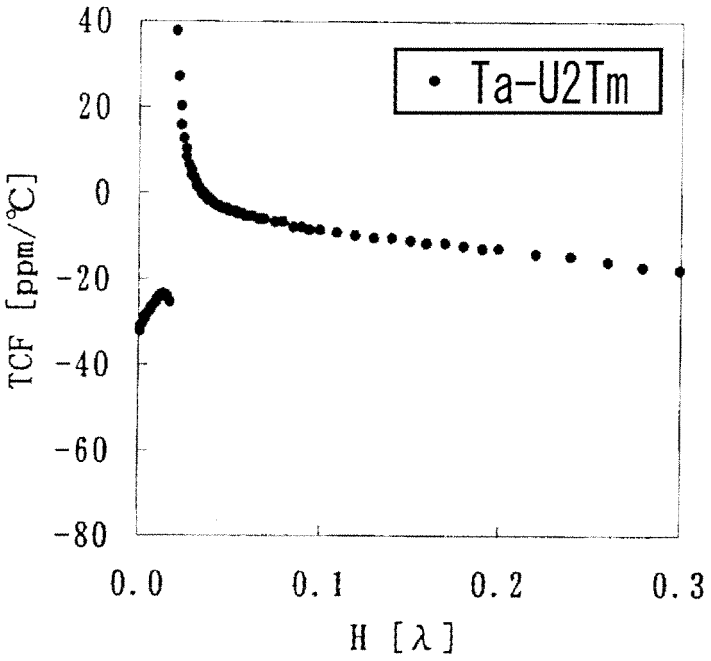
40
20
0
-20
-40
-60
-80
TCF [ppm/℃]
• Ta-U2Tm
0.0
0.1
0.2
0.3
H [λ]

FIG.48

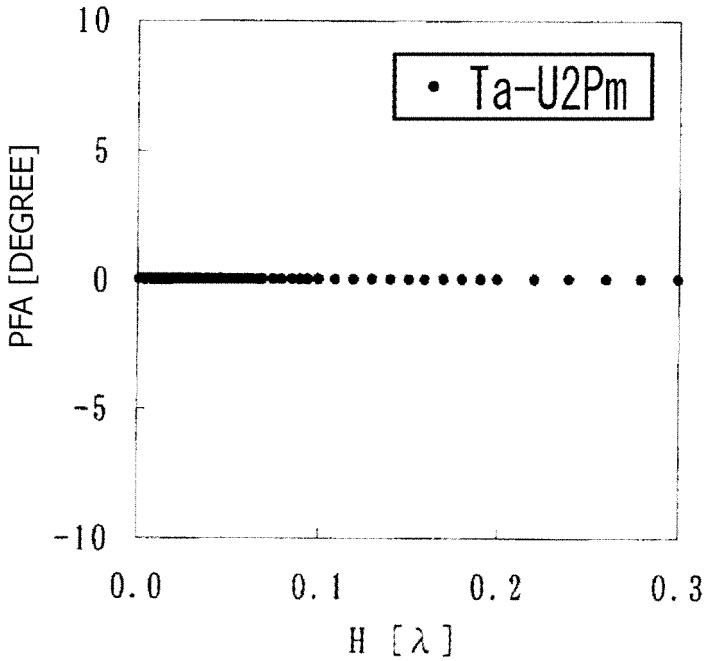
10
5
0
-5
-10
PFA [DEGREE]
• Ta-U2Pm
0.0
0.1
0.2
0.3
H [λ]

FIG.49

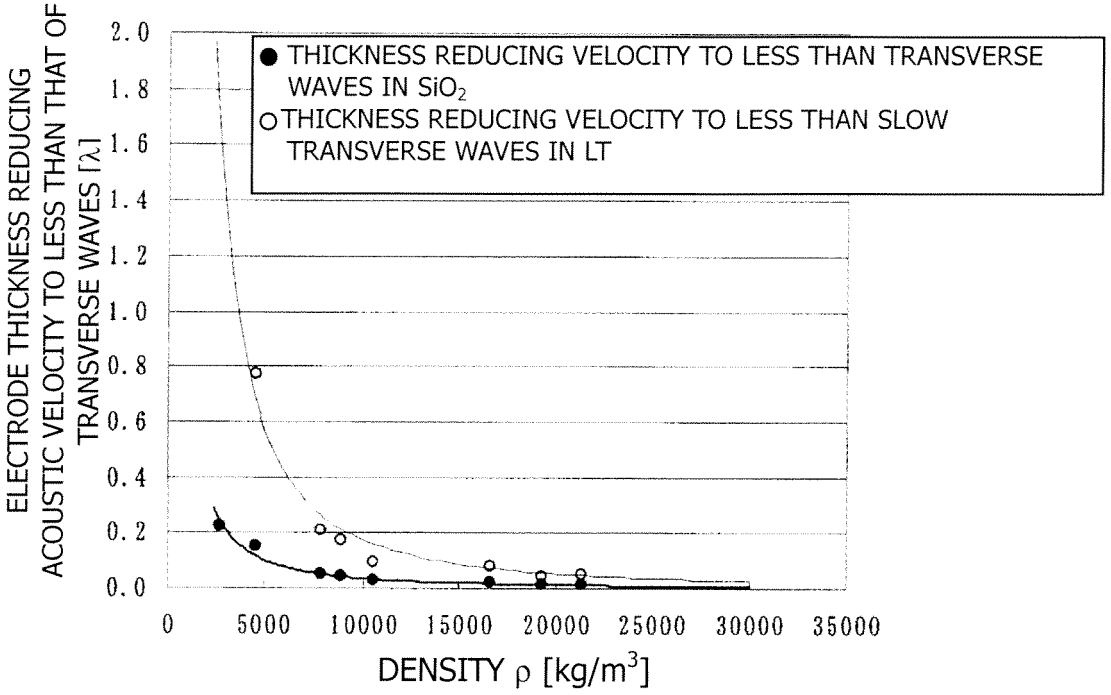
ELECTRODE THICKNESS REDUCING ACOUSTIC VELOCITY TO LESS THAN THAT OF TRANSVERSE WAVES [λ]
2.0
1.8
1.6
1.4
1.2
1.0
0.8
0.6
0.4
0.2
0.0
0
5000
10000
15000
20000
25000
30000
35000
DENSITY ρ [kg/m3]
● THICKNESS REDUCING VELOCITY TO LESS THAN TRANSVERSE WAVES IN SiO2
○ THICKNESS REDUCING VELOCITY TO LESS THAN SLOW TRANSVERSE WAVES IN LT

INTERNATIONAL SEARCH REPORT

International application No.
PCT/JP2005/003518

A. CLASSIFICATION OF SUBJECT MATTER
Int.Cl[7] H03H9/145, H01L41/09, 41/18, H03H9/25

According to International Patent Classification (IPC) or to both national classification and IPC

B. FIELDS SEARCHED

Minimum documentation searched (classification system followed by classification symbols)
Int.Cl[7] H03H9/145, H01L41/09, 41/18, H03H9/25

Documentation searched other than minimum documentation to the extent that such documents are included in the fields searched
Jitsuyo Shinan Koho 1922-1996 Jitsuyo Shinan Toroku Koho 1996-2005
Kokai Jitsuyo Shinan Koho 1971-2005 Toroku Jitsuyo Shinan Koho 1994-2005

Electronic data base consulted during the international search (name of data base and, where practicable, search terms used)

C. DOCUMENTS CONSIDERED TO BE RELEVANT

Category*	Citation of document, with indication, where appropriate, of the relevant passages	Relevant to claim No.
Y	WO 1998/52279 A1 (Hitachi, Ltd.), 19 November, 1998 (19.11.98), Claims 1, 8, 12; pages 5 to 13; Figs. 5, 12 (Family: none)	1-11
Y	JP 2002-152003 A (Murata Mfg. Co., Ltd.), 24 May, 2002 (24.05.02), Par. Nos. [0019], [0062] (Family: none)	1-11
Y	JP 2001-251157 A (Fujitsu Ltd.), 14 September, 2001 (14.09.01), Claim 1; Par. No. [0028] & JP 09-167936 A & JP 2000-315934 A & JP 2001-077663 A & US 006037847 A1 & US 006317015 B1 & DE 019641662 A & DE 019641662 A1 & CN 001159100 A	1-11

☒ Further documents are listed in the continuation of Box C. ☐ See patent family annex.

* Special categories of cited documents:
"A" document defining the general state of the art which is not considered to be of particular relevance
"E" earlier application or patent but published on or after the international filing date
"L" document which may throw doubts on priority claim(s) or which is cited to establish the publication date of another citation or other special reason (as specified)
"O" document referring to an oral disclosure, use, exhibition or other means
"P" document published prior to the international filing date but later than the priority date claimed
"T" later document published after the international filing date or priority date and not in conflict with the application but cited to understand the principle or theory underlying the invention
"X" document of particular relevance; the claimed invention cannot be considered novel or cannot be considered to involve an inventive step when the document is taken alone
"Y" document of particular relevance; the claimed invention cannot be considered to involve an inventive step when the document is combined with one or more other such documents, such combination being obvious to a person skilled in the art
"&" document member of the same patent family

Date of the actual completion of the international search	Date of mailing of the international search report
14 April, 2005 (14.04.05)	10 May, 2005 (10.05.05)
Name and mailing address of the ISA/ Japanese Patent Office Facsimile No.	Authorized officer Telephone No.

Form PCT/ISA/210 (second sheet) (January 2004)

INTERNATIONAL SEARCH REPORT

International application No.
PCT/JP2005/003518

C (Continuation). DOCUMENTS CONSIDERED TO BE RELEVANT

Category*	Citation of document, with indication, where appropriate, of the relevant passages	Relevant to claim No.
Y	JP 2003-258594 A (Murata Mfg. Co., Ltd.), 12 September, 2003 (12.09.03), Par. Nos. [0063] to [0074]; Fig. 1 & US 2003-0132684 A1 & EP 001324487 A2 & CN 001430330 A	6-11
Y	JP 6-350377 A (Hitachi, Ltd.), 22 December, 1994 (22.12.94), Par. Nos. [0008] to [0011], [0020]; Fig. 1 (Family: none)	6-11

Form PCT/ISA/210 (continuation of second sheet) (January 2004)

REFERENCES CITED IN THE DESCRIPTION

This list of references cited by the applicant is for the reader's convenience only. It does not form part of the European patent document. Even though great care has been taken in compiling the references, errors or omissions cannot be excluded and the EPO disclaims all liability in this regard.

Non-patent literature cited in the description

- Piezoelectric Acoustic Boundary Waves Propagating Along the Interface Between SiO2 and LiTaO. *IEEE Trans. Sonics and Ultrason.,* 1978, (6 **[0008]**
- Highly Piezoelectric Boundary Waves propagating in Si/SiO2/LiNbO3 Structure. *26th EM Symposium,* May 1997, 53-58 **[0009]**
- Highly Piezoelectric SH-type Boundary Waves. *IEICE Technical Report,* 1966, vol. 96 (249), 21-26 **[0010]**
- **OZAWA ; YAMADA ; OMORI ; HASHIMOTO ; YAMAGUCHI.** Production of boundary acoustic wave device by bonding substrate. *Piezoelectric materials and Device Symposium, 2003, Piezoelectric materials and Device Symposium Executive Committee,* 27 February 2003, 59-60 **[0011]**
- **J. J. CAMPBELL ; W. R. JONES.** A method for estimating optimal cuts and propagation directions for excitation and propagation directions for excitation of piezoelectric surface waves. *IEEE Trans. Sonics and Ultrason.,* 1968, vol. SU-15, 209-217 **[0059]**
- Acoustic Wave Device Technology Handbook. Society for the Promotion of Science, Acoustic Wave Device Technology the 150th Committee. 30 November 2001, 549 **[0077]**
- *Journal of the Acoustical Society of Japan,* 1980, vol. 36 (3), 140-145 **[0079]**